doi.org/10.1002/cptc.202000014

VIP *Very Important Paper*

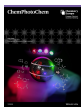

Heterogeneous Photocatalysis in Organic Synthesis

Sebastian Gisbertz[a, b] and Bartholomäus Pieber*[a]

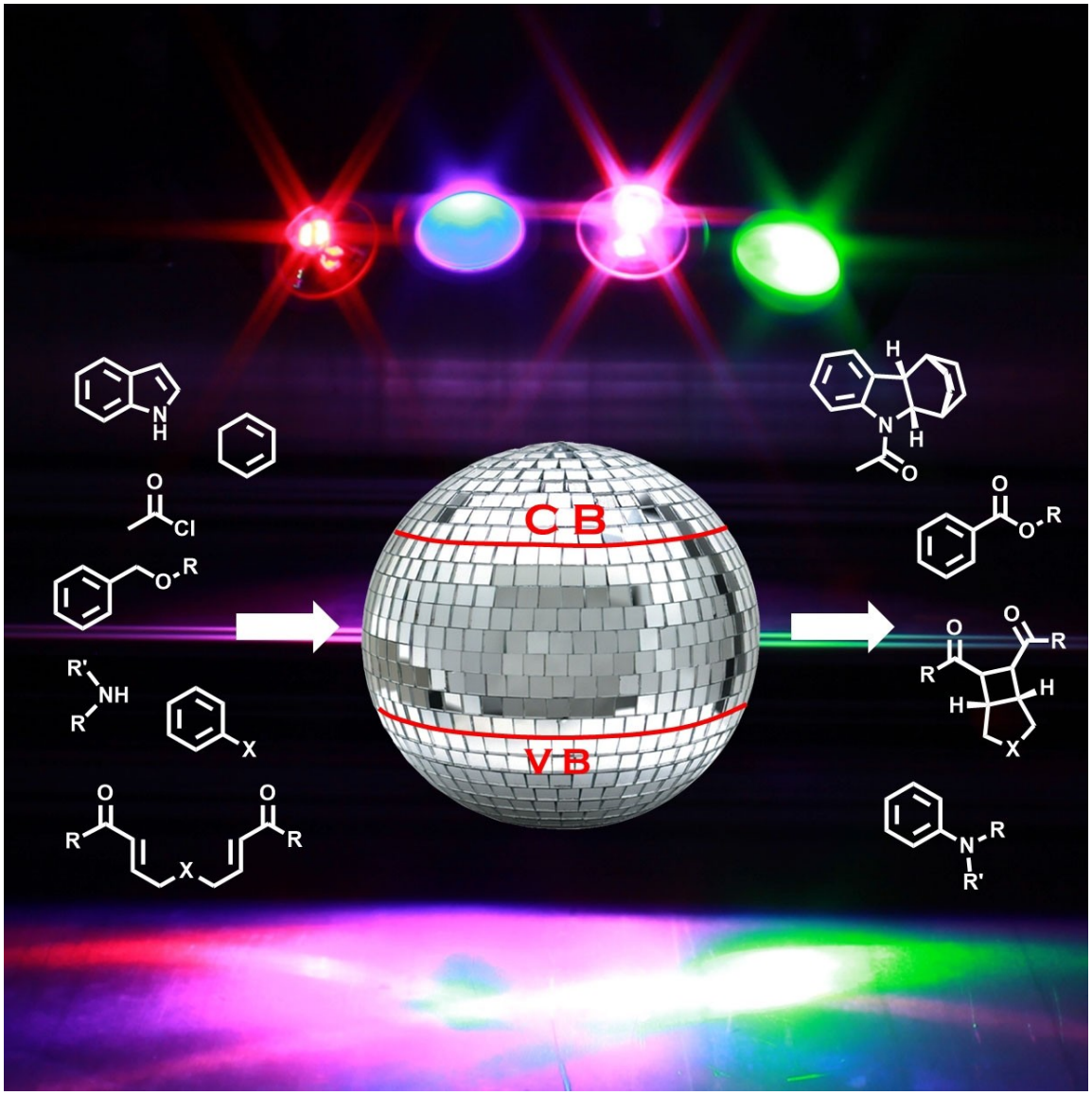

Visible light photocatalysis relies mainly on expensive noble metal complexes and organic dyes that are not recyclable. Heterogeneous semiconductors, which are mainly applied for artificial photosynthesis and wastewater treatment, are a promising sustainable alternative and gain increasing attention. Inorganic and organic semiconductors with suitable bandgaps are among the most widely studied heterogeneous photocatalysts due to their high stability and recyclability. More recently, microporous materials, such as conjugated organic polymers, covalent organic frameworks, and metal organic frameworks that can be tuned and designed on a molecular level showed promising results. This review provides an overview of the most common heterogeneous photocatalysts with a focus on their applicability in organic synthesis.

1. Introduction

Catalysis is a fundamental pillar of organic synthesis and is key to the production of commodity chemicals, complex pharmaceuticals, and agrochemicals. Catalysts are classified as either homogenous or heterogeneous. Homogeneous catalysis is, compared to heterogeneous catalysis, often characterized by a higher activity and selectivity.[1] Heterogeneous catalysts, on the contrary, can easily be separated and recycled. Combining the advantages of homogeneous and heterogeneous catalysis by anchoring soluble catalysts on insoluble supports is an appealing strategy,[1] but adds complexity to the catalytic system and often reduces the catalysts' activity and selectivity, or even result in complete deactivation. Heterogenized catalysts have often failed to outperform their soluble analogs and to achieve the potential of merging heterogeneous and homogeneous catalysis.[2]

In contrast to "conventional" catalysis (transition metal catalysis, organocatalysis, or Lewis acid catalysis), visible-light photocatalysis proceeds *via* electron or energy transfer to generate reactive intermediates of substrates or reagents rather than lowering the transition state energy.[3] Irradiation of a PC, typically a homogeneous ruthenium or iridium polypyridyl complex, results in an excited species that can accept or donate a single electron, enabling photoredox catalysis (PRC) *via* oxidative or reductive quenching cycles (Figure 1, A). An excited photocatalyst can alternatively also transfer its excited state energy (EnT) to a substrate or reagent to induce chemical reactions.[4] Heterogeneous photocatalysts, such as semiconductors, are operating by the same electron and energy transfer processes as homogeneous photocatalysts (Figure 1, B).[5] This is in stark contrast to conventional catalysis, where homogeneous catalysts cannot be simply substituted by a heterogeneous material. When a semiconductor absorbs photons with sufficiently high energy, electrons are excited from the valence band (VB) to the conduction band (CB), generating simultaneously an oxidizing and a reducing species on a single particle. The generated electron holes (h^+) can oxidize electron donors whereas the electrons in the VB are able to reduce electron acceptors *via* single-electron transfer.

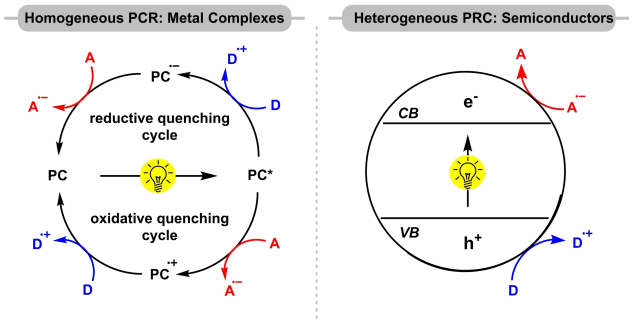

Figure 1. Homogeneous and heterogeneous photoredox catalysis.

This review provides an overview of the most common, purely heterogeneous photocatalysts, that were successfully applied in organic synthesis focusing on catalysts and strategies that enable the use of visible light (>400 nm). Our discussion includes "traditional" semiconductors (such as TiO_2), conjugated microporous polymers (CMPs), covalent organic frameworks (COFs), and metal organic frameworks (MOFs). Examples of homogeneous photocatalysts that are immobilized on supports are not discussed.[6] Mechanistic discussions of the individual reactions and the photoelectronic properties of semiconducting materials are out of the scope of this review and can be found elsewhere.[3,5,7]

2. Metal Oxides: TiO_2

Titanium dioxide is a naturally occurring mineral that has various applications ranging from the use as white pigment in dyes or cosmetics to its employment as photocatalyst for water purification or energy conversion.[7f] Although the large band gap semiconductor requires ultraviolet (UV) light irradiation to form electron-hole pairs, it is among the most frequently applied heterogeneous photocatalysts in organic synthesis.[7a] As the use of TiO_2 and other metal oxide semiconductors as PCs in organic synthesis was recently surveyed in an excellent review articles,[7a,8] we limit our discussion to a representative set of examples.

[a] *S. Gisbertz, Dr. B. Pieber*
Department of Biomolecular Systems
Max Planck Institute of Colloids and Interfaces
Am Mühlenberg 1, 14476 Potsdam (Germany)
E-mail: bartholomaeus.pieber@mpikg.mpg.de
Homepage: http://www.mpikg.mpg.de/catalysis
[b] *S. Gisbertz*
Department of Chemistry and Biochemistry
Freie Universität Berlin
Arnimallee 22, 14195 Berlin (Germany)

The radical decarboxylation of carboxylic acids, results in carbon-centered radicals, and can be initiated using UV(A) irradiation (>365 nm) in the presence of TiO_2 P25. This is the most commonly applied form of TiO_2 in photocatalysis and consists of the polymorphs anatase and rutile a ratio of 8:2. Under anhydrous, anaerobic conditions, the resulting stabilized carbon-centered radicals were coupled with N-substituted maleimides in moderate yields (Scheme 1).[9] In case of aryloxy-acetic acids (**1**), mixtures of the desired radical addition product (**3**) and chromene derivatives (**4**), which are generated in a photocatalytic addition-cyclization cascade, were observed.

Irradiation with UV-light is, however, often associated with severe drawbacks as high-energy photons can cause selectivity issues by, for example, activating substrates or reagents directly. To overcome such issues, strategies that enable the utilization of visible light are intensively investigated.

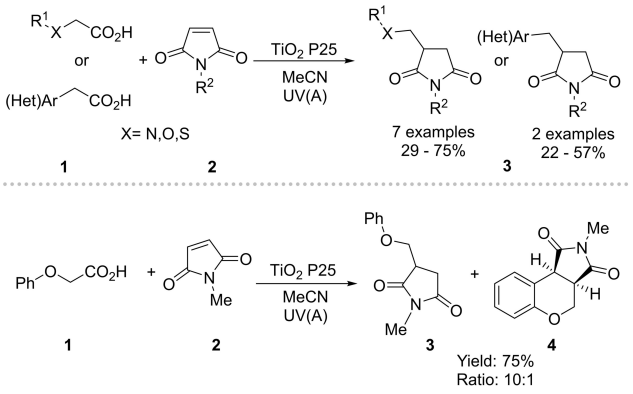

Scheme 1. Decarboxylative addition of carboxylic acids to *N*-substituted maleimides using TiO_2 and UV-light irradiation.[9]

2.1. Surface Complexation of Substrates/Reagents and TiO_2

A straightforward, but limited strategy that is able to extend the absorption of TiO_2 to visible light is the formation of a surface complex between TiO_2 and a heteroatom-containing substrate that creates a new electron donor level above the VB of the metal oxide (Figure 2).[5b]

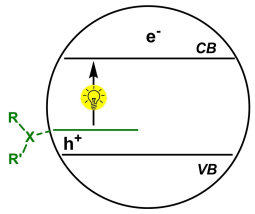

Figure 2. The formation of surface complexes between substrates and TiO_2 enables visible light harvesting.

Rueping and co-workers used this approach for the Meerwein-arylation of heteroaromatic compounds (**6**) with aryldiazonium salts (**5**) catalyzed by TiO_2 P25 (Scheme 2).[10] Mechanistic investigations indicated that a TiO_2–diazoether species (**8**), which absorbs visible light, is initially formed. The catalytic method enabled the arylation of furan, thiophene and pyridine in good to excellent yields.

The same group reported on a TiO_2 P25 catalyzed multi-component Ugi-type reaction of *N,N*-dimethylanilines (**9**) with isocyanides (**10**) and water that results in the formation of α-amino amides (**11**, Scheme 3).[11] The formation of a surface complex between the aniline derivative (**9**) and TiO_2 was proposed to be responsible for visible light absorption. The metal oxide semiconductor was recycled five times without any loss in catalytic activity.

Surface interactions between N,N,N′,N′-tetramethylethylenediamine (TMEDA) and TiO_2 enabled the synthesis of symmetrical and unsymmetrical disulfides (**14**) from thiols (**12, 13**) using visible light (Scheme 4, A).[12] The reaction rate was significantly increased in a continuous flow[13] approach using a packed bed reactor. To avoid high-pressure drops due to

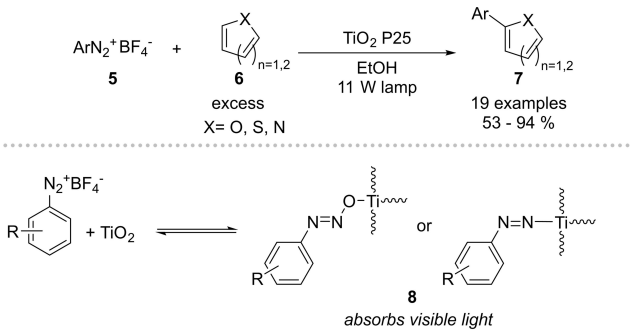

Scheme 2. Meerwein arylation of heterocycles catalyzed by TiO_2 using visible light *via* the formation of a TiO_2-diazoether complex.[10]

Sebastian Gisbertz studied chemistry in Aachen (Germany), where he obtained his Bachelor (2015) and Master (2018) degrees. In 2018, he moved to the Max-Planck Institute of Colloids and Interfaces as a Ph.D. candidate under the supervision of Dr. B. Pieber. His research interests include heterogeneous materials as photoredox catalysts, with a strong focus on carbon–heteroatom coupling reactions.

Dr. Bartholomäus Pieber studied chemistry in Graz (Austria) and received his Ph.D. in 2015 under the supervision of Professor C. Oliver Kappe in the field of multiphasic continuous flow chemistry. He subsequently moved to the Max-Planck Institute of Colloids and Interfaces for postdoctoral work, and was promoted to Group Leader in 2018. His research interests include photocatalysis, heterogeneous catalysis, reaction and catalyst development, mechanistic investigations and flow chemistry.

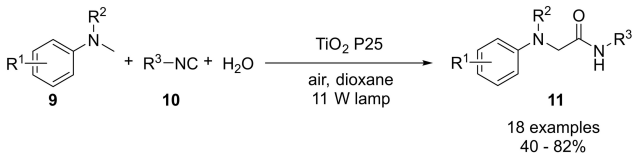

Scheme 3. Photocatalytic Ugi-type reaction using TiO_2 and visible light.[11]

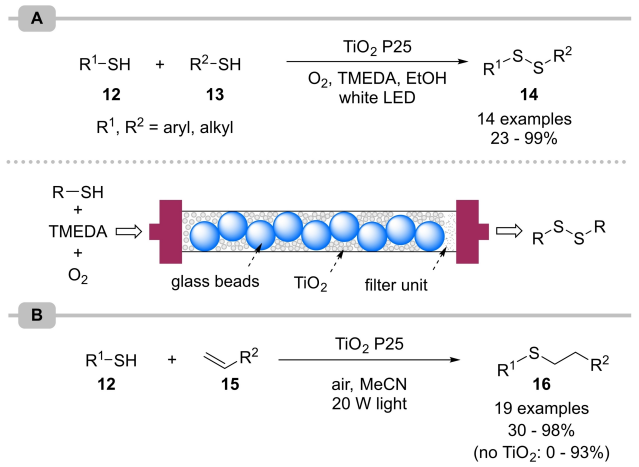

Scheme 4. (A) Disulfide formation and (B) thiol-ene reaction *via* SET oxidation of thiols by TiO_2 using visible light.[12–14]

aggregation of TiO_2 nanoparticles in the presence of TMEDA, glass beads were added as inert packing material.

Visible-light mediated thiol-ene reactions were shown to benefit from the presence of TiO_2 P25 (Scheme 4, B).[14] Binding of the thiol starting materials is likely responsible for the ability to use visible light as energy source. Although product formation was also observed in the absence of a catalyst in some cases, the efficiency and scope of this transformation was significantly increased when catalytic amounts of the heterogeneous semiconductor were added.

The groups of Scaiano and Yoon showed that a TiO_2–indole surface complex (**21**) can be excited with a 460 nm light source to promote the radical Diels-Alder reaction between indoles (**17**) and 1,3-cylcohexadienes (**18**) (Scheme 5).[15] To prevent

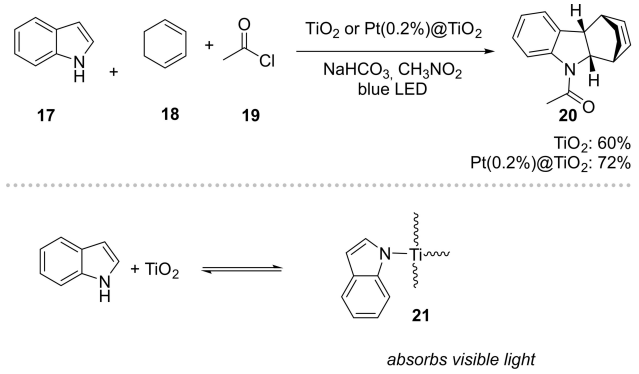

Scheme 5. Radical Diels-Alder reaction catalyzed by TiO_2 using visible light.[15]

fragmentation of the cycloaddition products, the reaction was carried out in presence of acetyl chloride (**19**) resulting in the desired acetylated tetrahydrocarbazoles (**20**). Platinum-doped titanium dioxide (Pt(0.2%)@TiO_2) was shown to double the photon efficiency in comparison to undoped TiO_2, and a range of protected tetrahydrocarbazoles (**20**) was synthesized in moderate to good yield.[16] During a recycling study, a decrease in the activity of Pt(0.2%)@TiO_2 was observed. The authors hypothesized that surface poisoning from organic compounds, most likely derived from indole, is responsible for catalyst deactivation.

2.2. Dye-Sensitized TiO_2

While surface complexation results only in a small redshift of the absorption of TiO_2, decoration of the metal oxide semiconductor with sensitizers (dyes) extends the absorption to a broader range of the visible light spectrum. This strategy is applied in dye-sensitized solar cells (DSSCs),[17] and dye-sensitized photocatalysts (DSPs) for light driven H_2 production.[18] Various functional groups are well established for the immobilization of dyes on TiO_2 in DSSCs including carboxylic acids, phosphonic acids, or sulfonic acids and various binding modes can be responsible for immobilization.[19] In most cases, an electron of the dye/sensitizer (sens) is excited from the HOMO to the LUMO, followed by injection into the CB of the semiconductor (type I sensitization, Figure 3). A "direct" electron-injection from the HOMO of the sensitizer into the semiconductor's CB upon photoexcitation is the basis of type II sensitization.[20] This mechanism is analogous to metal-to-ligand charge-transfer (MLCT) in ruthenium and iridium polypyridyl complexes, and a new absorption band is formed upon binding. In both cases, the valence band position is irrelevant for light harvesting, as photons are absorbed by the sensitizer. This avoids side reactions caused by highly reactive holes that would result from direct semiconductor excitation with UV light.

Zhao and co-workers sensitized TiO_2 with alizarin red (ARS@TiO_2) for the aerobic, photocatalytic oxidation of alcohols (**22**) in presence of catalytic amounts of 2,2,6,6-tetramethylpiperidine-1-oxyl (TEMPO, Scheme 6, A).[21] The sensitized semiconductor is proposed to remove an electron from TEMPO, generating $TEMPO^+$ that subsequently oxidizes the alcohols (**22**) to the corresponding aldehydes (**23**). Regeneration of the resulting TEMPO–H by the dye or O_2 closes the catalytic cycle.

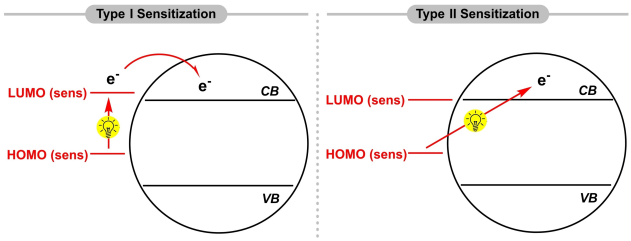

Figure 3. Sensitization of TiO_2.

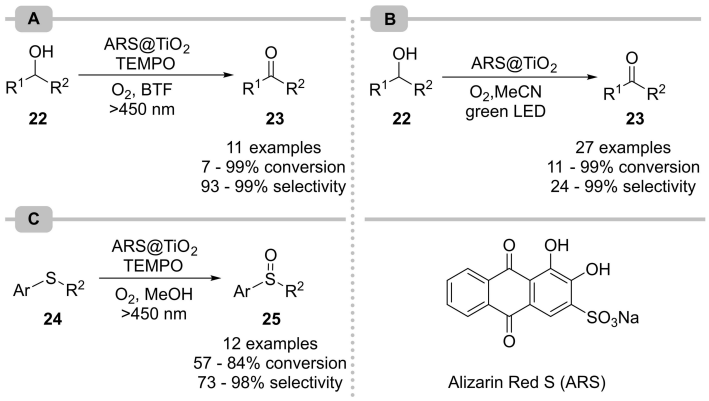

Scheme 6. Aerobic oxidation of alcohols (A, B) and sulfides (C) using ARS@TiO_2 as photocatalyst.[21,23,24]

A similar system was presented using eosin Y as sensitizer.[22] More recently, Lang and co-workers showed that the reaction works also efficiently in the absence of TEMPO (Scheme 6, B).[23] The combination of ARS@TiO_2 and TEMPO was also applied for the photocatalytic oxidation of sulfides (**24**) to sulfoxides (**25**) in the presence of oxygen (Scheme 6, C).[24] TEMPO was shown to be crucial for the stability of the photocatalyst as its addition avoids photodegradation of ARS.

Eosin Y sensitized TiO_2 (EoY@TiO_2) enabled the aerobic oxidation of benzyl ethers (**26**) to the corresponding benzoate esters (**27**) in moderate to excellent yield (Scheme 7).[25] The method tolerates various functional groups and is applicable to benzyl protected amino acids and carbohydrates.

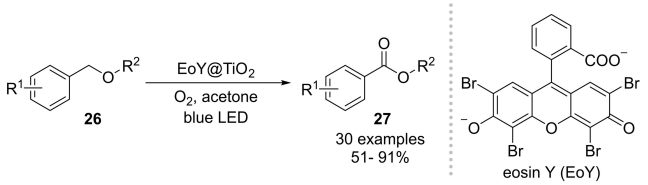

Scheme 7. Aerobic oxidation of benzyl ethers catalyzed by eosin Y sensitized TiO_2.[25]

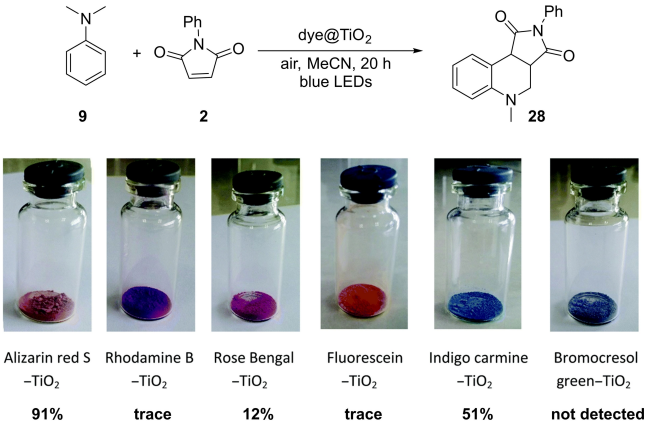

Scheme 8. TiO_2 sensitized with different dyes for the aerobic oxidative cyclization of *N,N*-dimethylaniline with *N*-phenyl maleimide. Reproduced with permission from Ref. [25], copyright American Chemical Society **2017**.

A comparison of various sensitizers immobilized on TiO_2 showed that ARS is well suited for a photocatalytic cascade radical C–C bond formation/cyclization of *N,N*-dimethylaniline (**9**) with *N*-phenylmaleimides (**2**) that results in **28** (Scheme 8).[26] A decreased catalytic activity was observed during recycling experiments and could be correlated to a decrease of the amount of the dye due to leaching.

Opatz and colleagues designed a type II sensitizer by merging a chromophore with a redox-active catechol surface anchoring group.[27] The resulting 6,7-dihydroxy-2-methylisoquinolinium (DHMIQ) was anchored on TiO_2 nanoparticles (DHIMQ@TiO_2) and showed a high activity as photocatalyst for the oxidative cyanation of tertiary amines (**29**) using trimethylsilyl cyanide (TMSCN, Scheme 9). The sensitized semiconductor was shown to harvest near-infrared (NIR) light, enabling the reaction even using a 730 nm light source.

Photocatalysis can be combined with other catalytic strategies, such as organocatalysis (dual catalysis).[28] König and co-workers showed that TiO_2 sensitized with Phos-Texas Red (PoTeRed@TiO_2) can be used as PC in combination with catalytic amounts of an imidazolidinone organocatalyst (**34**) for the visible-light-promoted α-alkylation of octanal (**32**) with diethyl bromomalonate (**31**) resulting in enantioenriched **33** (ee = 81%) in 65% (Scheme 10, A).[29] More recently, the group of Jang combined TiO_2 sensitized with a ruthenium dye (N719@TiO_2) with asymmetric iminium catalysis using visible light irradiation (Scheme 10, B).[30] The authors were able to perform highly enantio- and diastereoselective tandem Michael addition/oxyaminations of α,β-unsaturated aldehydes (**35**) with **36**.

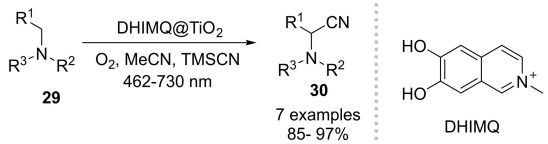

Scheme 9. Photocyanation of amines using TiO_2 decorated with a type II sensitizer.[27]

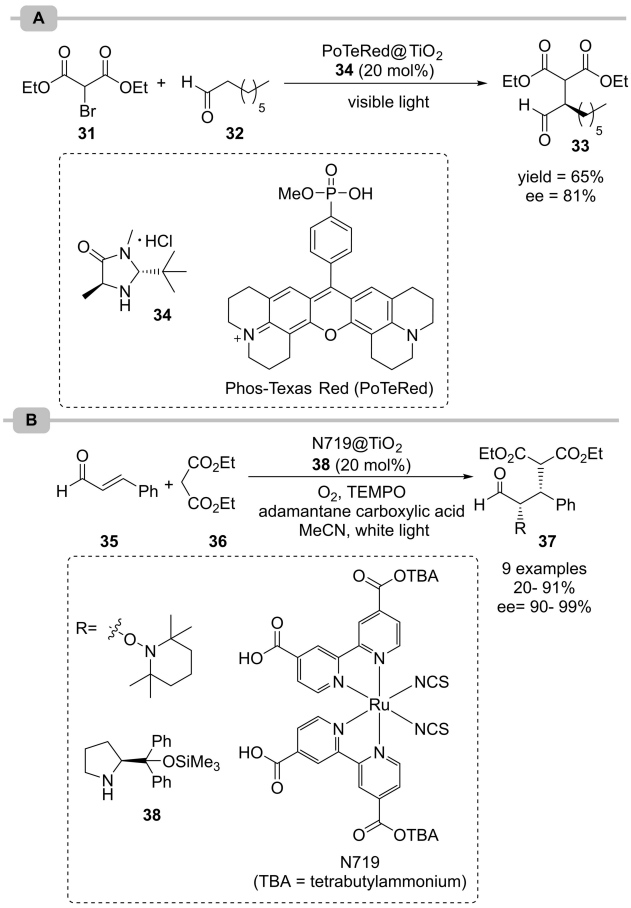

Scheme 10. Combination of sensitized TiO_2 and organocatalysis. (A) Visible-light-promoted α-alkylation of octanal with diethyl bromomalonate. (B) Tandem Michael addition/oxyaminations of α,β-unsaturated aldehydes.[29,30]

2.3. Metal-Doped TiO_2

Another possibility to extend the absorption of metal oxide semiconductors is metal doping *via* chemical or physical methods.[7f] Modifying TiO_2 with metal nanoparticles can narrow the band gap, and increase the photocatalytic activity due to an improved charge separation, as well as the reduction of electron-hole recombination rates.

Shen and co-workers showed that the surface modification of TiO_2 with nickel(II) oxide results in a material that absorbs visible light and is able to induce the photocatalytic cascade radical C–C bond formation/cyclization of *N,N*-dimethylanilines (**9**) with *N*-phenylmaleimides (**2**, Scheme 11).[31] The red shift upon surface modification is attributed to a rise of the valence band potential resulting from metal doping. Importantly, the photocatalyst did not show any reduction in its activity over nine cycles during a recyclability study.

By decorating TiO_2 with samarium oxide nanoparticles, Scaiano and co-workers developed a single material (Sm_xO_y@TiO_2) that can be used for dual photo/Lewis acid catalyzed intramolecular [2 + 2] cycloadditions of symmetrical aryl (bis)enones (**39**, Scheme 12).[32] The desired cycloadducts (**40**–**42**) were formed in moderate to good yield (47–72%)

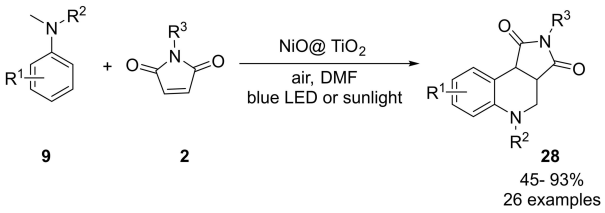

Scheme 11. Photocatalytic cyclization of tertiary anilines with maleimides using NiO doped TiO_2.[31]

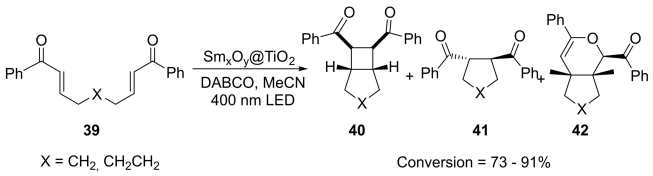

Scheme 12. Dual Photo/Lewis acid catalysis with a single bifunctional nanomaterial.[32]

using 400 nm LEDs. The same system was also used for the photoreductive cyclization of chalcones. Reusability studies showed no loss of efficiency over five cycles for the photoreductive coupling of chalcones.

Gold nanoparticles (Au NPs) absorb visible light due to the surface plasmon resonance effect. The Au NPs can be excited with visible light, leading to an injection of the excited electrons into the CB of TiO_2, which can be subsequently transferred to an electron acceptor.[5b] This strategy was used for the dimerization of benzyl bromides (**43**) using green light (Scheme 13).[33] Studies with the radical trap TEMPO suggest that the mechanism proceeds *via* a benzyl radical intermediate. A decrease in the catalytic activity during a recyclability study was related to a growth of the Au particles from 2.5 to 4.1 nm.

TiO_2 decorated with palladium nanoparticles (NPs) was used for the photocatalytic Ullmann cross-coupling of an electron-rich (**45**) and an electron-poor (**46**) aryl iodide (Scheme 14).[34] Interestingly, only the combination of UVA (368 nm) and blue (465 nm) light resulted in a relatively selective formation of the desired cross-coupling product (**47**). If only blue light was used, almost no conversion was observed whereas UVA light alone suffered from low selectivity. The authors concluded that the Pd NPs capture the electrons from the conduction band after excitation with UVA light, thereby increasing the lifetime of the electron-hole pair. Blue light is proposed to be exclusively absorbed by Pd NPs, initiating a final photoreductive elimination. Recyclability studies showed

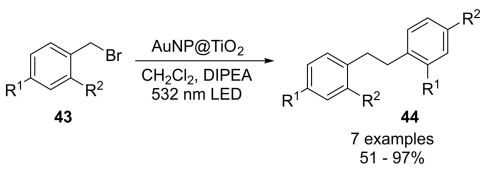

Scheme 13. Reductive dimerization of benzyl bromides using AuNP@TiO_2 and green LED irradiation.[33]

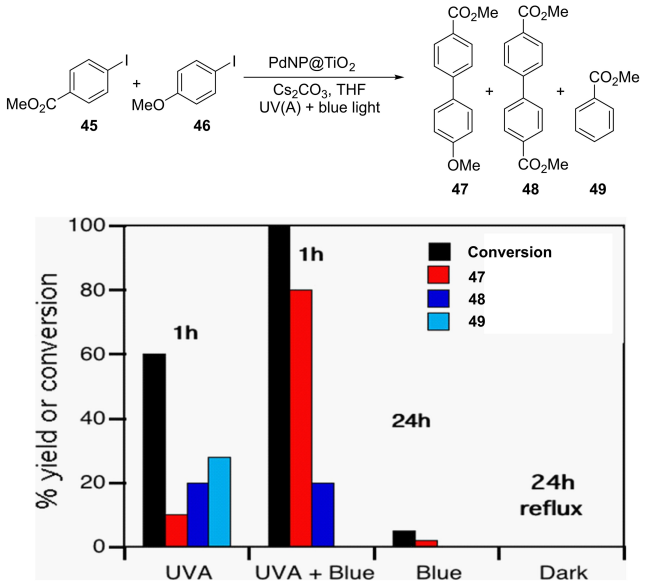

Scheme 14. Selectivity control in the photocatalytic Ullmann C–C coupling with palladium-doped TiO_2 using combined UVA and blue light. Reproduced with permission from Ref. [34], copyright American Chemical Society **2018**.

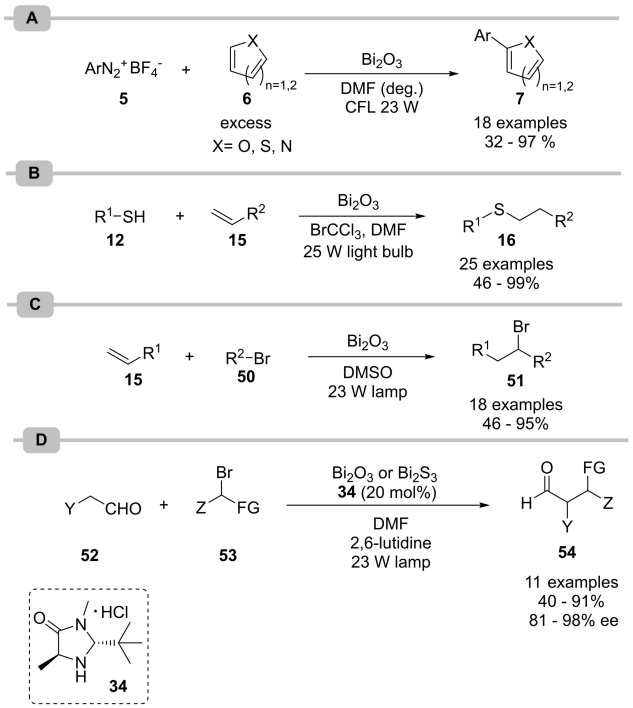

Scheme 15. (A) Meerwein arylation of heterocycles using Bi_2O_3 as photocatalyst.[36] (B) Thiol-ene reaction *via* SET oxidation of thiols by Bi_2O_3 using visible light.[37] (C) Atom-Transfer radical addition of bromo ATRA donors to olefins using Bi_2O_3 as visible light photocatalyst.[38] (D) Visible-light-promoted α-alkylation of aldehydes with α-bromocarbonyl compounds combining organocatalysis and Bi_2O_3 as visible light photcatalyst.[39]

that the conversion stays constant over four cycles, whereas the selectivity decreases.

The same group used Pd NPs on TiO_2 for light-mediated Sonogashira couplings.[35] In this case, the photocatalyst lost its catalytic activity completely after two cycles. Since ICP-OES analysis showed no Pd leaching, catalyst poisoning by alkyne hydrogenation products on the surface was proposed as a plausible reason.

3. Bismuth Oxide

Bismuth(III) oxide has a smaller band gap (2.1–2.8 eV) than TiO_2 and absorbs visible light without the need for any modifications. Pericàs and co-workers showed that catalytic amounts of Bi_2O_3 catalyze the Meerwein-type coupling of aryl diazonium salts (**5**), which were generated in-situ from anilines, with heteroaromatic compounds (**6**) suing visible light irradiation (Scheme 15, A).[36]

Fadeyi and colleagues used Bi_2O_3 for late-stage diversifications of complex biomolecules and active pharmaceutical ingredients via photocatalytic thiol-ene reaction using $BrCCl_3$ as radical source.[37]

The visible light-induced atom-transfer radical addition (ATRA) of alkyl radicals to olefins was also reported using this versatile metal oxide photocatalyst (**15**, Scheme 15, C).[38] Here, the photoexcited state of Bi_2O_3 is capable to promote the cleavage of the C–Br bonds (of the ATRA donors) to form the alkyl radicals.

Similarly, alkyl radicals generated via Bi_2O_3 photocatalyzed C–Br bond cleavage were used for the enantioselective α-alkylation of aldehydes (**52**) in presence of a second-generation imidazolidinone catalyst (**34**, Scheme 15, D).[39]

Other Bismuth based semiconductors, such as Bi_2WO_6, $BiVO_4$, and BiOCl can be also used as visible light photocatalyst for, for example, the oxidation of alcohols,[40] toluene[41] or amines.[42]

4. CdSe, CdS

Cadmium sulfide and cadmium selenide are small band gap semiconductors that absorb visible light up to 540 nm. One of the main advantages of these materials is the straightforward preparation of colloidal nanocrystals (quantum dots, QDs). The optical properties, including the CB and VB position, can be tuned by modifying the nanoparticle size.[43]

CdSe QDs were used for the photocatalytic C–O bond cleavage of a model substrate (**55**) that emulates the depolymerisation of β-O-4-linkages that are found in lignin (Scheme 16).[44] An initial, thermal oxidation of **55** with Bobbitt's salt followed by the photocatalytic C–O bond cleavage yields 4-acetanisole (**57**) and guaiacol (**58**). The CdSe QDs (3.3 nm), that were stabilized by oleic acid and trioctylphosphine oxide, gave turnover numbers (TON) up to 128 000. A comparison with a molecular, homogeneous iridium photocatalyst ($[Ir(ppy)_2(dtbbpy)]PF_6$) showed that the QDs have a 15 times greater turnover frequency.

Weiss and colleagues reported on a stereoselective [2+2] cycloaddition of 4-vinylbenzoic acid derivatives (**59**, **60**) with

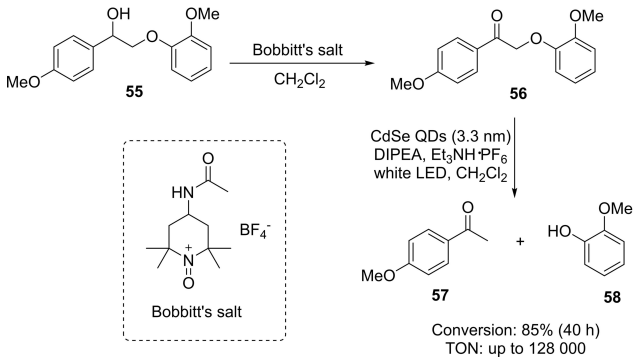

Scheme 16. Photocatalytic C–O cleavage of a lignin model structure using CdSe QDs.[44]

tunable regioselectivity using CdSe QDs that yields tetra-substituted *syn*-cyclobutanes (**61**, Scheme 17).[45] Transient absorption spectroscopy experiments indicated that the reaction proceeds *via* an energy transfer mechanism. The selectivity towards head-to-head products results from a reversible binding of the substrates/products *via* their carboxylic acid functionalities on the surface of the QDs. The authors proposed that the surface binding results in non-covalent π-π interactions between the rigid olefins that are responsible for the selective production of the kinetically disfavoured *syn*-products. Depending on the position of the acid functionality in the substrate, different regioisomers can be formed selectively. The ability to precisely control the triplet energy levels of the QDs by tuning the particle size further enabled challenging intermolecular hetero-cycloadditions.

Porous CdSe nanosheets with a thickness of 1.7 nm were used for the photocatalytic deuteration of aryl halides (**62**) *via* photocatalytic D_2O splitting in presence of Na_2SO_3 as sacrificial electron donor (Scheme 18, A).[46] Similarly, ZnSe/CdS-core/shell quantum dots, enabled the reductive dehalogenation of electron deficient (hetero)aryl halides (**64**) using visible light in presence of DIPEA (Scheme 18, B).[47] The radical intermediates can be also trapped with *N*-substituted pyrrole (**66**) to generate the respective C-C coupling products.

The versatility of CdSe QDs for photocatalytic organic synthesis was reported by Weix and co-workers.[48] The authors showed that single-sized CdSe QDs (3.0 ± 0.2 nm), stabilized by trioctylphosphine oxide and oleic acid, are efficient catalysts for a range of photoredox reactions including the β-alkylation of aldehydes, the β-aminoalkylation of ketones and the dehalogenation of aryl iodides. The authors further showed that the

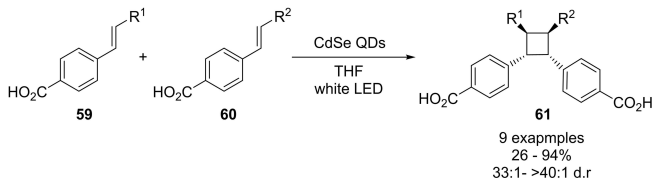

Scheme 17. Regio- and stereoselective [2 + 2] cycloaddition of 4-vinylbenzoic acid using CdSe QDs under visible light irradiation.[45]

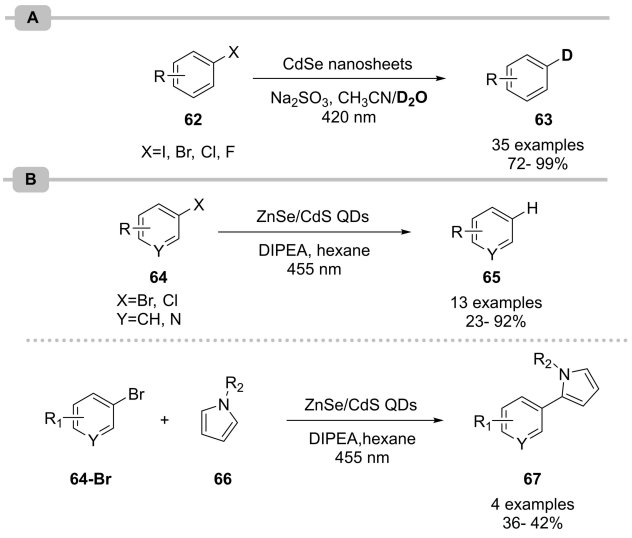

Scheme 18. (A) Deuteration of aryl halides by photocatalytic D_2O water splitting with porous CdSe sheets as photocatalyst.[46] (B) Reductive dehalogenation of aryl halides and C–H arylation with pyrroles using ZnSe/CdS core/shell quantum dots as photocatalyst.[47]

heterogeneous semiconductor is able to act as photocatalyst for the amination of aryl halides in combination with nickel catalysis (Scheme 19, A). Similarly, Xiao and co-workers used CdS in combination with nickel catalysis for C–N and C–O cross-couplings (Scheme 19, B).[49] Moderate to excellent yields were obtained for the coupling of various amines (**71**) and alcohols (**73**) with electron-poor aryl bromides (**62-Br**). The heterogeneous photocatalyst could be recycled ten times without significant loss in activity.

Weiss and colleagues demonstrated that tuning the ligand shell of CdS QDs can increase the reaction rate for the photocatalytic C–C coupling of 1-phenylpyrrolidine (**75**) and

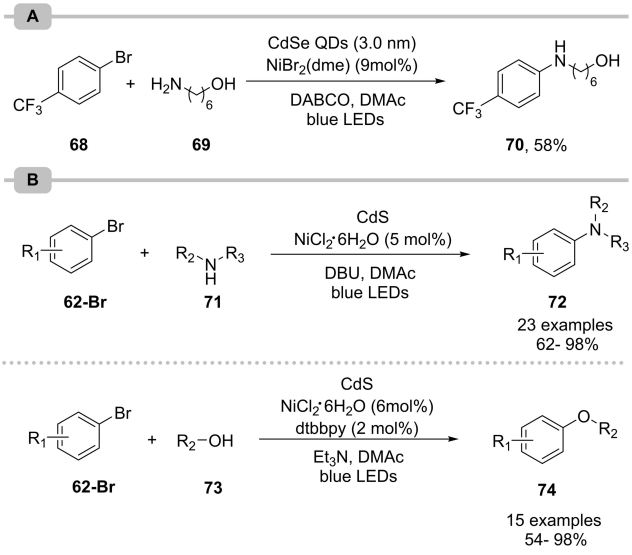

Scheme 19. Dual photo/nickel catalysis using semiconductors. (A) C–N cross-coupling using CdSe QDs. (B) C–N and C–O cross-couplings using CdS.[48,49]

phenyl *trans*-styryl sulfone (**76**, Scheme 20).[50] Replacing a portion of the oleate ligand by octyl phosphonate creates a mixed monolayer that increased the initial rate by a factor of 2.3 compared to CdS QDs with an oleate ligand shell. This phenomenon is attributed to a better permeability of the ligand shell that facilitates the rate-limiting charge transfer between 1-phenylpyrrolidine (**75**) and the QD core.

The oxidative coupling of amines (**78**) was achieved using visible light irradiation and CdS nanosheets in the presence of oxygen (Scheme 21, A).[51] The high specific surface area (56.3 m^2/g) of the porous CdS nanosheets contributed to an better performance compared to CdS nanoparticles.

The transfer hydrogenation of *N*-benzylidenebenzylamine derivatives (**79**) that gives the respective dibenzylamines (**80**) was realized using 4-fluorothiophenol as hole acceptor and hydrogen atom donor using green LEDs or sunlight and CdSe/CdS core/shell quantum dots as photocatalysts (Scheme 21, B).[52]

5. Lead Halide Perovskites

Lead-halide perovskite ($APbX_n$) are promising materials for photochemical applications with tunable optical band gaps depending on, for example, the halide composition.[53] One of the few examples for the application of lead halide perovskites in organic synthesis is the photocatalytic formation of symmetrical and unsymmetrical disulfides (**14**) from thiols (**12, 13**) using $CsPbBr_3$ under aerobic conditions (Scheme 22, A).[54] The same catalytic system was also suitable for the light-mediated cross-dehydrogenative phosphonylation of *N*-aryl tetrahydroisoquinoline derivatives (**81**) or tertiary amines (**82**). Both reactions showed high efficiency and moderate to excellent

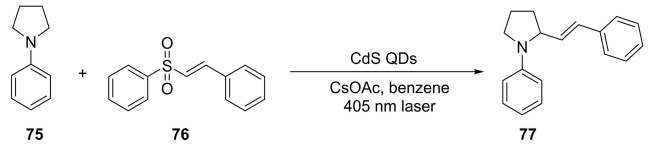

Scheme 20. Photocatalytic C–C coupling of 1-phenylpyrrolidine and phenyl trans-styryl sulfone using CdS QDs.[50]

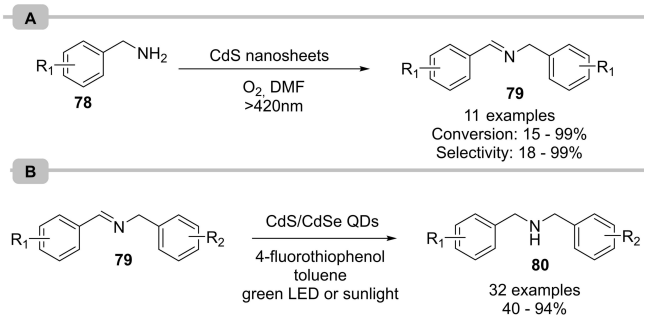

Scheme 21. (A) Photocatalytic oxidative coupling of benzyl amines to imines using CdS nanosheets. (B) Light-mediated transfer hydrogenation of *N*-benzylidenebenzylamine using core/shell CdS/CdSe QDs.[51,52]

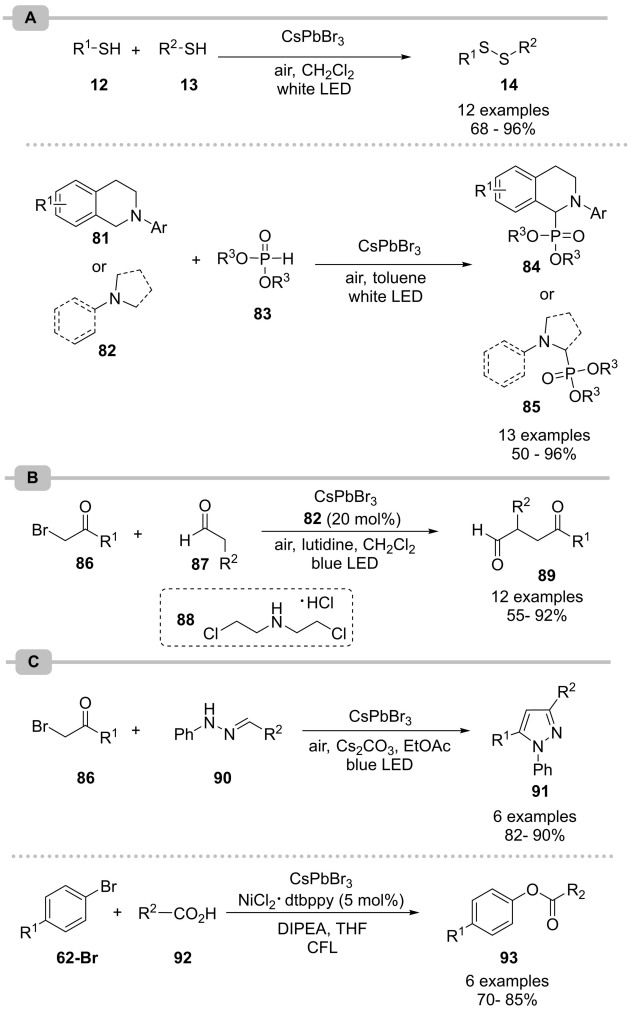

Scheme 22. (A) Disulfide formation and cross-dehydrogenative coupling between tertiary amines and phosphite esters using $CsPbBr_3$ as photocatalyst. (B) α-Alkylation of aldehydes using $CsPbBr_3$ as photocatalyst. (C) Photocatalytic pyrazole synthesis and dual nickel/photo catalyzed esterification using $CsPbBr_3$ as photocatalyst.[54–56]

yields (50–96%) were obtained. Changing bromine to iodine in the $CsPbX_3$ structure reduces the bandgap, but the lower oxidation potential led to lower photocatalytic activity towards the disulfide formation. $CsPbCl_3$, on the contrary, has a higher oxidative potential, but the large bandgap makes it unsuitable for visible light photocatalysis.

$CsPbBr_3$ was also used in combination with an amine organocatalyst for the α-alkylation of aldehydes (Scheme 22, B).[55] The catalytic system showed TONs over 52,000 for the α-alkylation of aldehydes (**87**), which is three orders of magnitude higher than for molecular Ir or Ru photocatalysts. The application of $CsPbBr_3$ was further expanded to a range of other photocatalytic transformations that include the formation of pyrazoles (**91**), and the dual photo/nickel catalyzed cross-coupling of aryl bromides (**62-Br**) and carboxylic acids (**92**, Scheme 22, C).[56]

6. Carbon Nitrides

Graphitic carbon nitrides (g-CN), a class of metal-free polymers, are among the most studied materials for heterogeneous photocatalysis.[57] The organic semiconductors absorb light in the visible area (bandgap ~2.7 eV). In general, g-CN polymers are easy to synthesize from readily available and cheap precursors, such as urea, cyanamide, or melamine. The band gap and position of the valence and conduction band depend on several factors such as the C/N ratio, the polymerization degree or the crystallinity that can be tailored *via* the synthetic approach. We limit our discussion about their use as photocatalysts to a selected set of examples, as the field was recently summarized in several reviews.[7b–d]

In a collaborative effort, the groups of Blechert, Wang and Antonietti pioneered the application of carbon nitride materials for synthetic purposes, showcasing the photocatalytic properties of these organic semiconductors for the oxidation of alcohols,[58] and amines.[59] The same groups further realized the photocatalytic aerobic dehydrogenative C–C coupling of *N*-aryl tetrahydroisoquinolines (**81**) with various nucleophiles (**94**), including nitroalkanes, dimethyl malonate and ketones using mesoporous graphitic carbon nitride (mpg-CN, Scheme 23, A).[60] This material is prepared using silica nanoparticles as templates to obtain a high surface area (200 m^2/g) that makes it ideally suited for catalytic applications. It was also used for the fluoroalkylation of (hetero)arenes (**96**) *via* the generation of CF_3 radicals in the single electron reduction of trifluoromethanesulfonyl chloride (Scheme 23, B).[61]

The versatility of mpg-CN as photocatalyst for organic synthesis was recently demonstrated for a range of reactions, including the twofold C–H functionalization of heteroarenes (**96**, Scheme 24, A).[62] The authors further demonstrated the direct C–H functionalization using metal salts that enabled, for example, brominations, cyanations and thiocyanations of arenes (Scheme 24, B). The heterogeneous, organic semiconductor was also used as photocatalyst in combination with a homogeneous nickel catalyst for the semi-heterogeneous dual photoredox nickel catalytic aryl amination of aryl bromides with secondary and primary amines (Scheme 24, C).

Similarly, a carbon nitride that is prepared through co-condensation of urea and oxamide followed by post-calcination

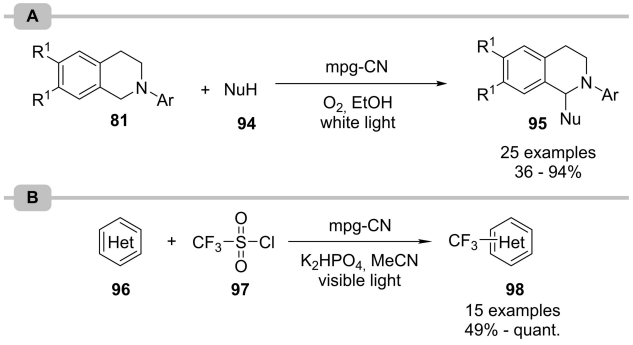

Scheme 23. (A) Cross-dehydrogenative couplings and (B) the fluoroalkylation of (hetero)arenes using mpg-CN as photocatalyst.[60-61]

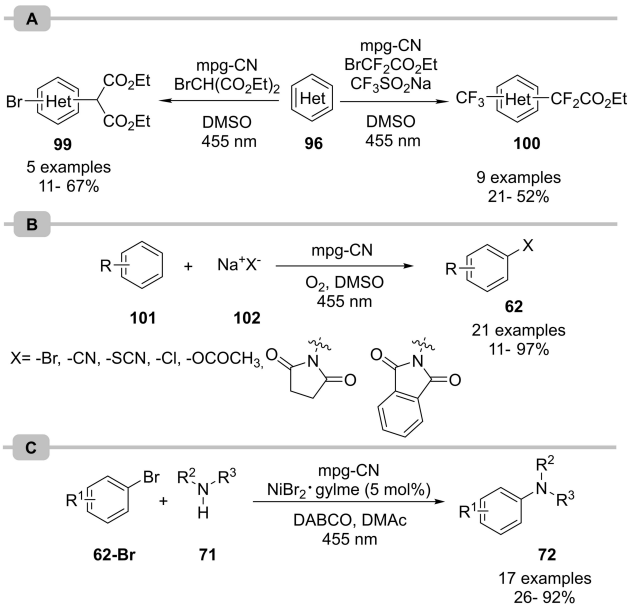

Scheme 24. (A) C–H bifunctionalization of arenes using mpg-CN. (B) C–H functionalization using alkali metal salts as nucleophiles. (C) Ligand-free mpg-CN/nickel dual catalytic C–N cross-couplings of aryl bromides amines.[62]

in a molten salt (CN–OA-m) proved efficient for dual nickel/photocatalysis.[63] The semi-heterogeneous approach enabled the esterification and (thio)etherification of electron-poor aryl halides (**62**, Scheme 25, A). In these cases, the heterogeneous semiconductor could be reused several times without any loss in reactivity. Real-time monitoring of the esterification by *in situ* FTIR spectroscopy showed that the kinetic profile of the carbon nitride catalyzed protocol is similar to the reaction using homogeneous iridium photocatalysis.[63a] Using a similar protocol the corresponding C–N cross-coupling did also enable the coupling with aryl halides that lack an electron withdrawing group, but suffered from severe reproducibility issues.[63c] The reactions frequently resulted in low yields and the heterogeneous, yellow PC became black. High amounts of deposited

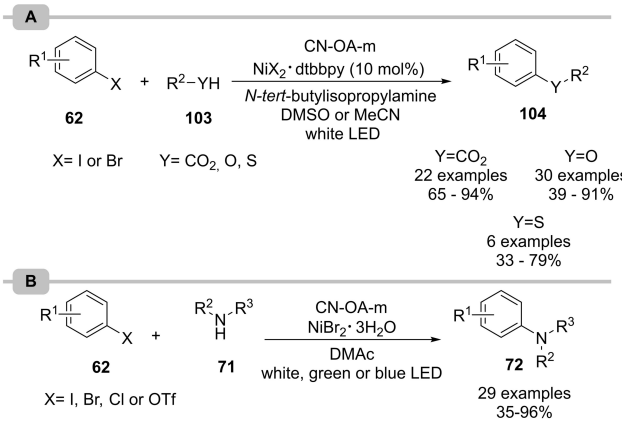

Scheme 25. Dual photo/nickel-catalyzed carbon–heteroatom cross-couplings using CN–OA-m. (A) Esterification and thio(etherification) of aryl halides and (B) amination of aryl halides.[63]

nickel were detected on the recovered carbon nitride by ICP-OES analysis, indicating nickel-black formation. In addition, recycling of the heterogeneous PC was not successful: the yellow CN–OA-m turned dark green after three cycles due to nickel deposition and the amine formation decreased significantly. The authors demonstrated that these problems can be avoided by controlling the reactivity of the carbon nitride photocatalyst using higher wavelengths, or reducing catalyst-solvent interactions.

A graphitic carbon nitride that was prepared by pyrolysis of guanidine hydrochloride was used to generate α-aminoalkyl radicals *via* desilylative and decarboxylative photocatalytic single electron oxidations of α-silylamines (**105**) and α-amino acids (**106**, Scheme 26).[64] The resulting radicals were applied for the addition to alkenes, as well as allylations and heteroarylations. Other semiconductors (TiO_2, $BiVO_4$) did not show any activity towards the desired products under identical conditions. The authors further showed that the heterogeneous semiconductor does not lose its catalytic activity upon recycling.

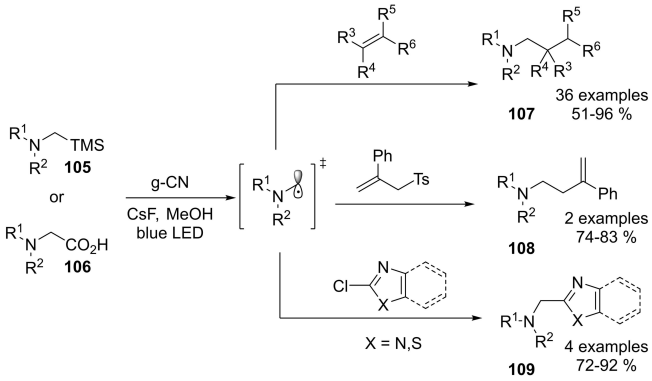

Scheme 26. Desilylative and decarboxylative generation of α-aminoalkyl radicals using g-CN.[64]

Reisner and co-workers showed that a cyanamide functionalized carbon nitride (NCN–CN) has a significantly higher activity than homogeneous Ir/Ru photocatalysts in the photocatalytic Minisci-type reaction of electron-deficient *N*-heteroarenes (**110**) with alcohols, amides, and cyclic ethers (Scheme 27).[65] While no reaction was observed in the absence of O_2, the addition of Pt nanoparticles enabled the coupling under anaerobic conditions. The evolution of hydrogen indicated that the Pt NPs consume the generated electrons *via* proton reduction. The same functionalized carbon nitride material was used for the sulfonylation of alkenes where it also outperformed other photocatalysts, including eosin Y and other CN derivatives.[66]

A carbon nitride material that was synthesized from cyanuric acid, melamine and barbituric acid (CMB–CN) was used for the decarboxylative fluorination of phenoxyacetic acids (**113**) and phenylacetic acid derivatives using Selectfluor in a continuous flow approach (Scheme 28).[67] A packed-bed reactor was not suitable as carbon nitride semiconductors are opaque. Handling of solid materials in other flow reactor types is challenging and leads to clogging. To overcome this general limitation, the authors developed a dedicated reactor system.

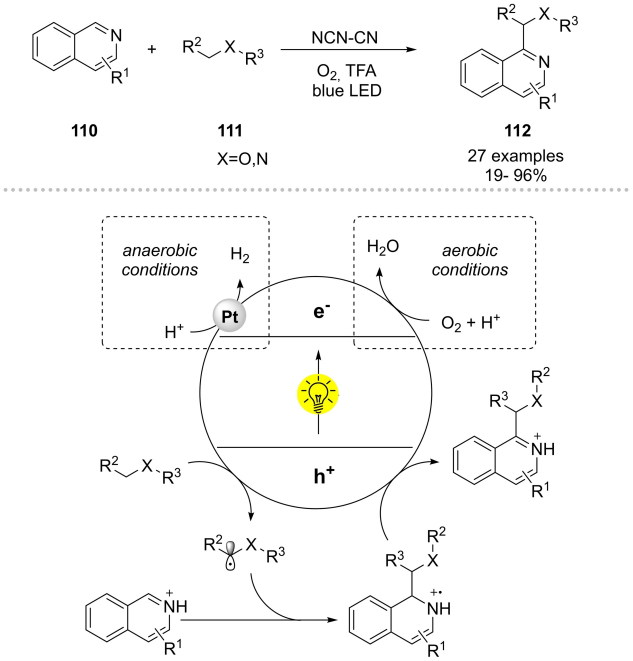

Scheme 27. Minisci-type coupling using carbon nitride catalysis.[65]

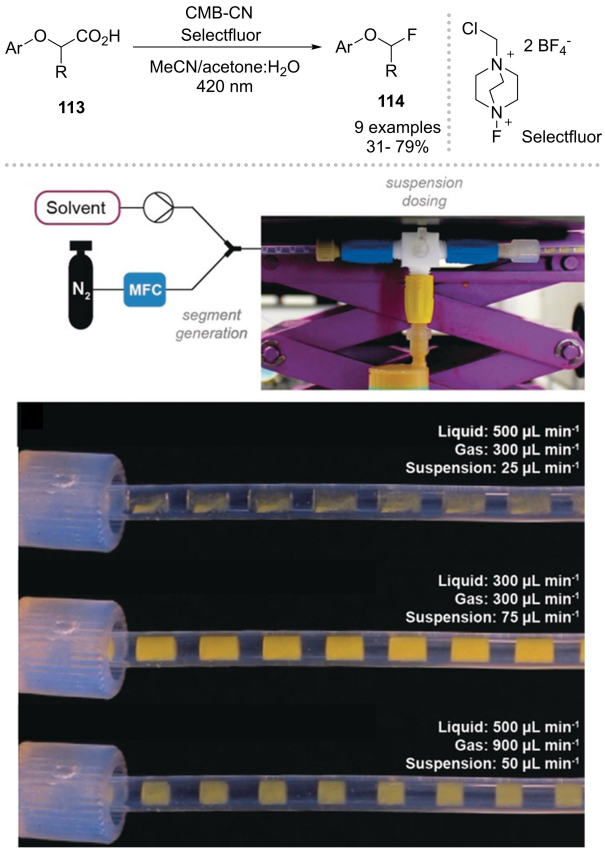

Scheme 28. Decarboxylative fluorination of phenoxy acid derivatives in continuous flow. Reproduced with permission from Ref. [67], copyright Wiley-VCH **2018**.

The key innovation was the introduction of a catalyst suspension into a gas–liquid slug stream. The resulting serial micro batch reactors (SMBRs) can be fed into an irradiated coil reactor that is submerged in a thermostatic bath. The natural Taylor flow mixes the slug to continuously re-suspend the material, ensuring efficient irradiation and reproducible processing. In this system, the reaction time can be adapted by changing the gas and/or liquid flow rate or the reactor volume while the catalyst stoichiometry can be varied by changing the rate of suspension dosing.

Potassium poly(heptazine imide), an ionic carbon nitride derivative with a high valence band potential of +2.54 eV *vs* RHE (g-CN: 1.82 eV *vs.* RHE), is perfectly suited for reactions that benefit from strong single electron oxidants. 1,3,4-oxadiazoles (**116**) can be effectively synthesized starting from *N*-acylhydrazones (**115**) using K–PHI as photocatalyst and S_8 as electron donor at 80 °C in nonpolar solvents (Scheme 29, A).[68] When the reaction was carried out at lower temperatures (50 °C), the rate decreased significantly and 43% instead of 80% yield were reached. Heating to 80 °C was also crucial for high reaction rates during the light-mediated, K–PHI catalyzed synthesis of 1,3-disubstituted-5,6-dihydropyrrolo[2,1-a]isoquinolines (DHIPQs, **119**) from tetrahydroisoquinolines (**117**) and chalcones (**118**) using blue light (Scheme 29, B).[69] Chalcones (**118**) can also be (cyclo)dimerized with K–PHI photocatalysis in the presence of TEOA (triethanolamine) as electron donor, resulting in cylcopentanoles (**120**, Scheme 29, C).[70] Performing these reactions at 80 °C increased not only the reaction rate, but also resulted in higher selectivities compared to lower temperatures, likely due to thermodynamic control in the formation of the five-membered ring.

7. Conjugated Microporous Polymers (CMPs)

Conjugated microporous polymers (CMPs) have a well-defined, conjugated backbone that can be rationally designed, allowing to tune their electrical and optical properties.[7e] These amorphous polymers have a highly porous structure that stems from the covalent connection of rigid, contorted molecules.

Poly(benzothiadiazoles) are among the most common CMPs applied in organic synthesis and were recently reviewed.[71] The versatile PCs are commonly synthesized *via* metal-catalyzed cross-couplings of benzothiadiazole (acceptor) and other aromatic (donor) monomer units. A poly(benzothiadiazole) CMP was, for example, used for the formation of singlet oxygen ($^1O_2$) and its utilization in the synthesis of ascaridole (**122**) from α-terpinene (**121**, Scheme 30, A).[72] The CMP (CMP–BTD) was synthesized by the polymerization of 4,7-dibromobenzo[c][1,2,5]thiadiazole with 1,3,5-triethynylbenzene *via* Sonogashira cross-couplings. SiO_2 nanoparticles were used as templates to increase the porosity of the polymeric materials. The BET surface was raised from 270 m^2/g for a CMP (no SiO_2 template) to 660 m^2/g, when 60 mg/mL SiO_2 nanoparticles were used. The high porosity and specific surface area were beneficial for an enhanced accessibility of the excited solid polymer for solubilized oxygen, leading to increased reaction rates. Using a continuous-flow system, a $^1O_2$ production of up to 1 mmol/min was measured with a maximum quantum yield of 0.06. More recently, a similar CMP was shown to be also applicable for the stereoselective [2+2] cycloaddition of styrene derivatives.[73]

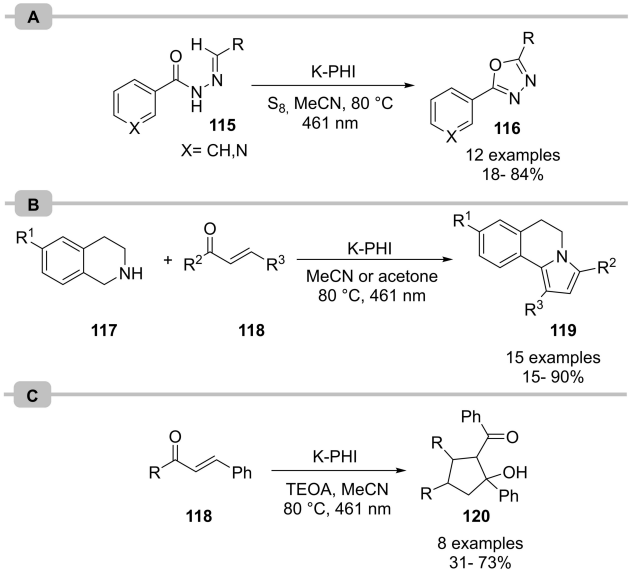

Scheme 29. (A) Photooxidation of N-acylhydrazones to 1,3,4-oxadiazoles with S_8 as oxidant and K–PHI as photocatalyst. (B) Oxidative condensation between tetrahydroisoquinolines and chalcone catalyzed by K–PHI. (C) Reductive cyclodimerization of chalcones using K–PHI as photocatalyst.[68–70]

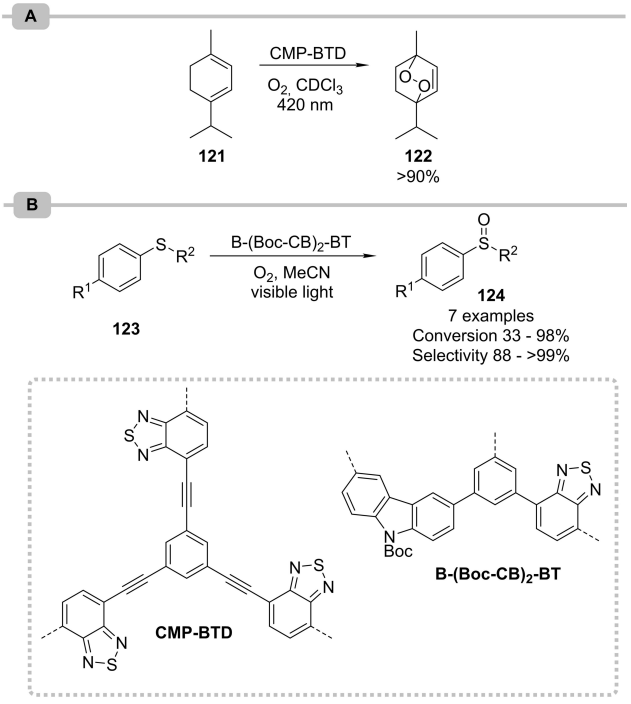

Scheme 30. (A) Oxidation of α-terpinene to ascaridole with poly(benzothiadiazole) conjugated porous polymer (CMP–BTD) as photocatalyst for the photocatalytic production of $^1O_2$. (B) Photocatalytic aerobic oxidation of aryl alkyl sulfides B-(Boc–CB)$_2$–BT.[72,74]

Zhang and co-workers synthesized a CMP *via* Suzuki-Miyaura-couplings of a benzothiadiazole monomer and a Boc-protected carbazole co-monomer using a high internal phase emulsion polymerization approach.[74] The resulting B-(Boc–CB)$_2$–BT was shown to be applicable as photocatalyst for the aerobic oxidation of aryl alkyl sulfides (**123**) to the corresponding sulfoxides (Scheme 30, B). The same reaction was also realized using a ferrocene-based CMP.[75]

A benzobisthiadiazole CMP (B_2–Fl_2–BBT) was prepared *via* Sonogashira couplings in high internal phase emulsion polymerization of a benzobisthiadiazole unit, a fluorene derivative, and 1,3,5-triethylenebenzene.[76] The resulting material showed a broad absorption range from visible to near-IR light and was applied as catalyst for the light-mediated debromination of α-bromoacetophenone derivatives (**125**) using Hantzsch ester as hydrogen donor and DIPEA as electron donor (Scheme 31).

A Friedel-Crafts alkylation was used to prepare a poly (benzothiadiazole) CMP (MOP-1) using formaldehyde dimethyl acetal (FDA) as bridging agent and 4,7-diphenylbenzo[c][1,2,5]-thiadiazole (BT–Ph_2) as photoactive unit (Scheme 32).[77] The photocatalytically active polymer with a BET surface of 586 m^2/g gave moderate to good yields for the bromination of electron rich aromatic compounds (**101**) using HBr in the presence of O_2.

Fine-tuning of the VB and CB band levels can be carried out by varying the amount of the benzothiadiazole monomers during the CMP preparation. This enables the facile synthesis of a library of CMP materials with different bandgaps. Zhang and co-workers used this approach to study the activity of different polybenzobisthiadiazoles based CMPs for the photocatalytic synthesis of a 1,2,3,4-tetrahydroquinoline derivatives (**28**) by a cascade radical C–C bond formation/cyclization of N,N-dimethylaniline (**9**) with *N*-phenylmaleimide (**2**, Scheme 33).[78]

Benzooxadiazoles can be also used to prepare photocatalytically active CMP materials. Similarly to the above examples using benzothiadiazole monomers, bandgap engineering *via* the synthetic approach is feasible. This was showcased for the preparation of CMPs with different substitution patterns using Sonogashira-type couplings of different alkynes with 4,7-dibromobenzo[c][1,2,5]oxadiazole (Scheme 34).[79] While the material resulting from a benzene co-monomer that contains four alkyne functionalities (B–BO-1,2,4,5) showed an excellent light harvesting behaviour with an absorption range up to near IR light, a CMP made using B–BO-1,3,5 had the highest catalytic activity for the aerobic oxidation

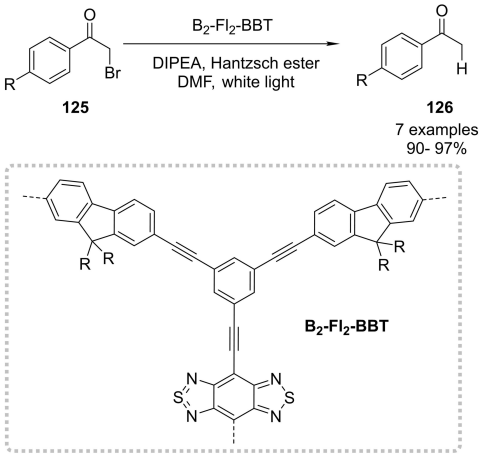

Scheme 31. Dehalogenation of haloketones using a poly-benzobisthiadiazole CMP as heterogeneous photocatalyst using visible light.[76]

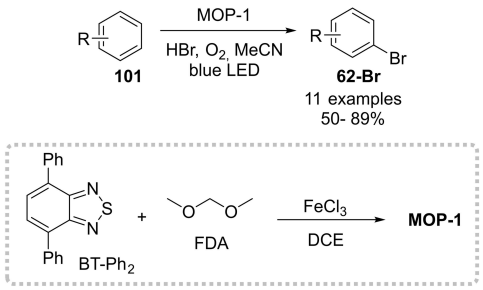

Scheme 32. Selective bromination of electron-rich aromatic compounds using microporous cross-linked organic polymers and HBr under blue light irradiation.[77]

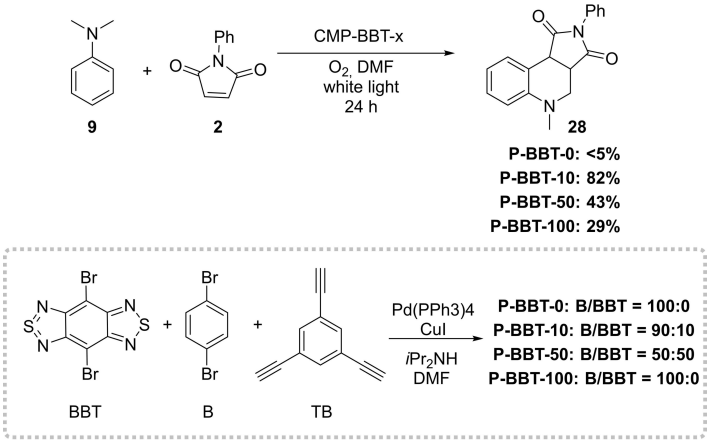

Scheme 33. Activity of different polybenzothiadiazoles based CMPs in the photocatalytic synthesis of 1,2,3,4-tetrahydroquinolines.[78]

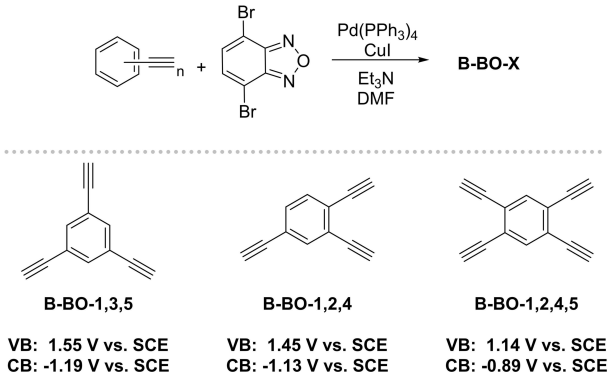

Scheme 34. Bandgap engineering by co-monomer variation during the synthesis of poly(benzooxadiazole) CMPs.[79]

of amines due to its higher conduction band potential. This same CMP was further decorated with Pd nanoparticles to enable light-mediated Suzuki cross-couplings.[80]

The oxidation of amines was used to showcase that truxene-based conjugated microporous polymer are photocatalytically active using visible light irradiation ($\lambda > 420$ nm) or natural sunlight.[81] Carbazolylic CMPs (Cz–CMPs), that were synthesized *via* Friedel-Crafts alkylations were applied as photocatalysts for the aerobic oxidation of amines and sulfides,[82] the dehalogenation of phenacyl bromides (**125**), the oxidative hydroxylation of aryl boronic acids (**127**), and the redox neutral α-functionalization of aldehydes in presence of an additional organocatalyst (**130**, Scheme 35).[83] It was further shown that the heterogeneous photocatalytic material could be reused without losing its catalytic activity.

A cationic, porous polycarbazole with incorporated, heteroleptic iridium polypyridyl units (CPOP-29) showed also good activity in the hydroxylation of aryl boronic acids and was further used for cross-dehydrogenative coupling of *N*-aryl tetrahydroisoquinoline derivatives (**81**) and several nucleophiles, such as phosphite esters and nitroalkanes (Scheme 36).[84] An enhanced activity was achieved by introducing CF_3 groups into the polymeric network, which led to superior light-absorption ability and a longer fluorescence lifetime.

An Eosin Y dye-based porous organic polymer (EY–POP-1) can also be used for aza-Henry reactions.[85] Eosin Y was polymerized with 1,3,5-triethinylbenzene to obtain an extended π-conjugation structure. Importantly, the CMP was recycled 12 times without loss in efficiency. Additionally, a difluoroborate-based conjugated microporous polymer (B–COP) was tested for the same reaction.[86] The polymeric material with a broad absorption band in the visible light region (400–700 nm) was synthesized by a base-catalyzed condensation polymerization between difluoroboron β-diketonate and tris(4-formylphenyl) amine.

A azulene–CMP (P–Az–B) enabled the visible-light mediated palladium-free Stille-type coupling of aromatic butyl stannanes (**131**) and aryl iodides (**62-I**) using white light (Scheme 37).[87] The method, however, works only for aryl halides that have strong electron-withdrawing substituents,

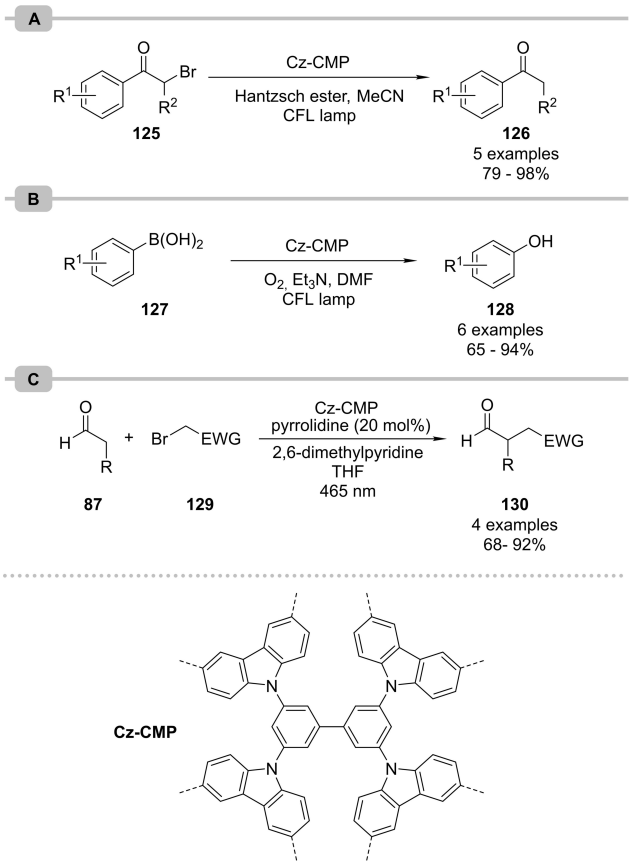

Scheme 35. A carbazole conjugated microporous polymer as photocatalyst for (A) the debromination of phenacyl bromides, (B) the hydroxylation of aryl boronic acid and (C) the alkyation of aldehydes.[83]

which was rationalized by the stabilization of the formed aryl radical anion.

Su and co-workers prepared a CMP *via* $FeCl_3$ catalyzed Friedel Crafts reactions of 4-CzIPN (1,2,3,5-Tetrakis(carbazol-9-yl)-4,6-dicyanobenzene), that is also a potent photocatalyst alone.[88] The recyclable catalyst absorbed up to 800 nm and had high thermal stability. Its photocatalytic activity was demonstrated for the generation of an alkoxyalkyl radical from 1,3-dioxolane that induces the 1,2-formylarylation of *N*-acrylamides (**133**), forming the corresponding 3-formyloxindole products (**135**, Scheme 38). The products were used for the construction of oxo-and aza-ring fused indolines and spirocyclic indole derivatives in thermal transformations.

8. Covalent Organic Frameworks (COFs)

Covalent organic frameworks (COFs) are two- or three-dimensional, highly ordered structures that are constructed by covalently linked building blocks.[89] In contrast to amorphous CMPs, COFs are crystalline, porous materials. The potential applications of COFs include gas storage and separation, drug delivery, energy storage, and the use as photocatalysts.

Covalent triazine networks (CTF), a subclass of COFs, were used for the aerobic oxidation of benzyl alcohols,[90] and the

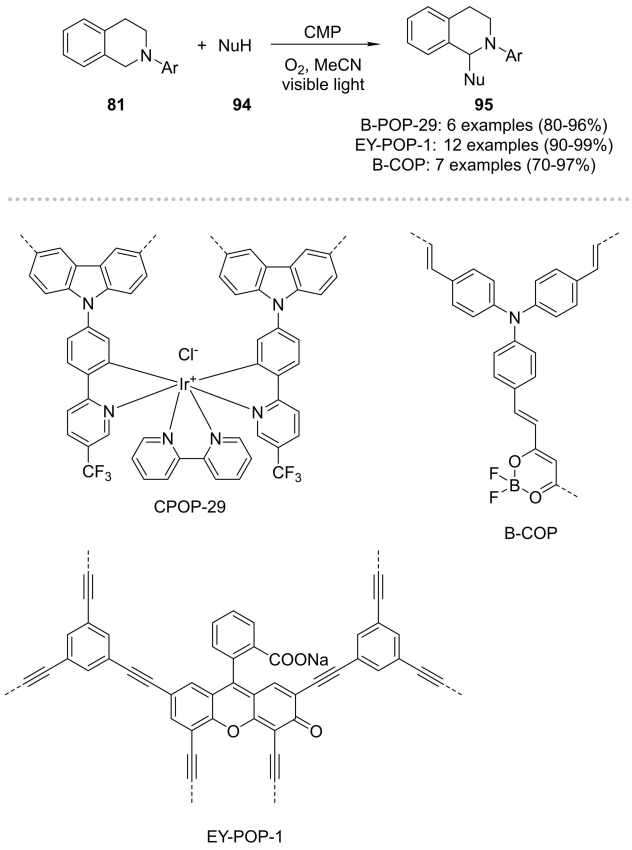

Scheme 36. Dehydrogenative C–H functionalization of *N*-aryl substituted tetrahydroisoquinoline derivatives using different conjugated porous polymers and visible light irradiation.[84]

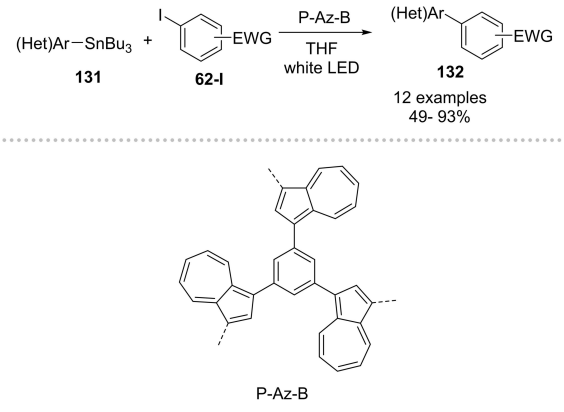

Scheme 37. Palladium-free Stille-type coupling using a conjugated microporous polymer and visible light irradiation.[87]

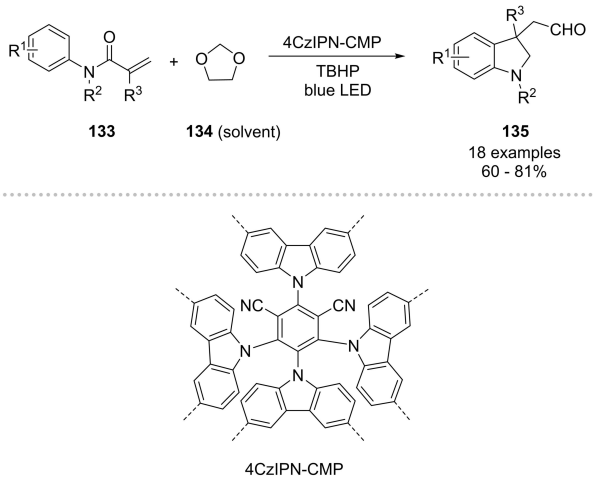

Scheme 38. Photocatalytic cascade radical cyclization of *N*-arylacrylamides *via* H-atom abstraction of 1,3-dioxalane using 4CzIPN–CMP as photocatalyst.[88]

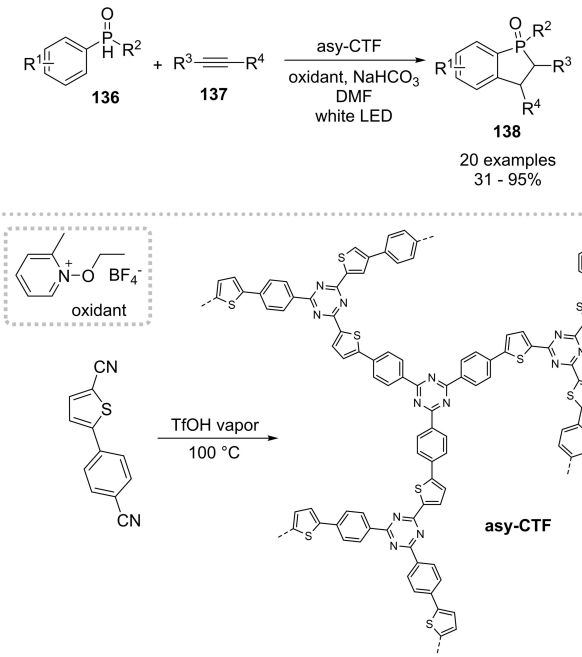

Scheme 39. Photocatalytic synthesis of benzophosphole oxides using a CTF.[92]

cross-dehydrogenative coupling of *N*-aryl substituted tetrahydroisoquinoline with nucleophiles.[91] More recently, an asymmetric CTF (asy-CTF), made *via* a TfOH-catalyzed trimerization of 5-(4-cyanophenyl)thiophene-2-carbonitrile, was used for the photocatalytic synthesis of benzophosphole oxides (**138**, Scheme 39).[92] The asymmetric donor-acceptor structure resulted in a higher activity than symmetrical analogues, which was rationalized by an enhanced charge separation and intramolecular electron transfer.

Yang and co-workers accessed a two-dimensional COF (2-D-COF-1) photocatalyst by the condensation of 2,5-dimethoxyterephtalohydrazide with 1,3,5-triformylbenzene (Scheme 40).[93] The highly crystalline and thermostable framework absorbs visible light up to ~700 nm and was shown to be a potent photocatalyst for the tandem radical-addition cyclization of 2-arylphenyl isocyanides (**139**) with alkyl and aryl hydrazines (**140**). The authors further showed that **140** can be replaced by other radical precursors such as CF_3SO_2Na, diphenylphosphine oxide or diphenylsulfide. Importantly, the heterogeneous PC was recycled six times maintaining its catalytic activity. The same COF structure was further shown to

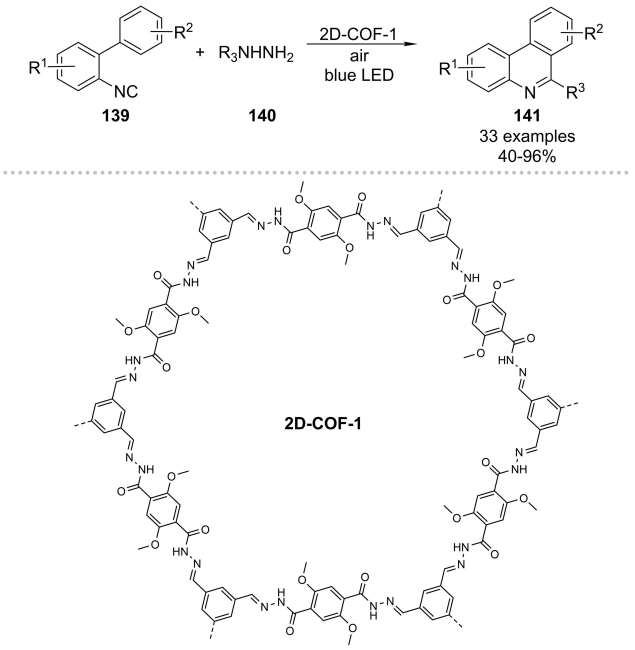

Scheme 40. Tandem radical-addition cyclization of 2-arylphenyl isocyanides with alkyl and aryl hydrazines using a hydrazine-based COF.[93]

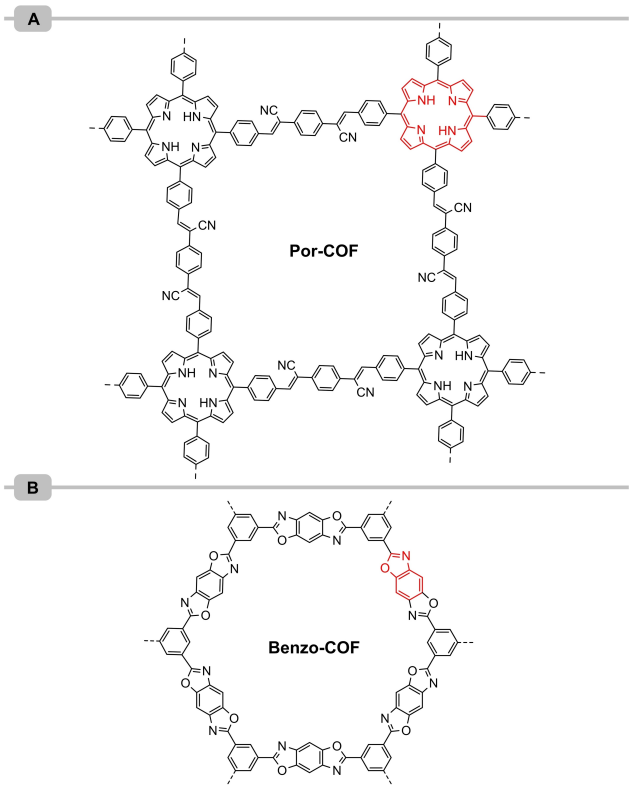

Scheme 41. Photocatalytically active covalent organic frameworks with incorporated porphyrin[95] (A) and benzoxazole (B) units.[96]

catalyze the cross-dehydrogenative coupling of *N*-aryl substituted tetrahydroisoquinoline with nucleophiles.[94]

Other examples of COFs that were successfully applied in photocatalysis are two-dimensional, porphyrin- (Por–COF),[95] and benzoxazole-based frameworks[96] (Benzo–COF; Scheme 41). The fully organic, heterogeneous PCs were used to activate O_2 for the aerobic photocatalytic hydroxylation of aryl boronic acids (Benzo–COF), and the oxidation of amines (Por–COF).

9. Metal Organic Frameworks (MOFs)

Metal organic frameworks (MOFs) are porous, highly ordered crystalline solids that consist of metal ions/cluster and organic linkers. In case of photocatalytically active MOFs, the metallic cluster (semiconductor), or a photocatalyst that is encapsulated in the pores of a photocatalytically inactive MOF can be responsible for their catalytic activity.[97] The vast majority of MOF photocatalysts, however, gain their photocatalytic activity from the incorporation of a molecular dye into the organic linker structure (Scheme 42). This can be, for example, accomplished, by using the ligand of Ru polypyridyl complexes as linker in combination with $ZrCl_4$ in presence of acetic acid (A).[98] Similarly an iridium polypyridyl complex serves as (metal) organic linker in a Zr–MOF.[99] Jiang and co-workers showed that porphyrin dyes can be combined with $ZrOCl_2 \cdot 8H_2O$ to obtain a photocatalytically active MOF (B).[100] Similarly, a porphyrin-based MOF can be obtained using indium metal clusters.[101] Zn-based MOFs were synthesized using a combination of bis(3,5-dicarboxyphenyl)pyridine and bis(3,5-dicarboxyphenyl)methylpyridinium (C).[102] All of these heterogeneous materials showed promising photocatalytic activity in reactions involving the generation of reactive oxygen species that were discussed in the previous chapters, including the oxidation of amines, the hydroxylation of arylboronic acids, and the dehydrogenative C–C coupling of *N*-aryl tetrahydroisoquinolines with various nucleophiles.

Duan and colleagues demonstrated that the incorporation of a photoactive polyoxometalate ($[SiW_{11}O_{29}Ru(H_2O)]^{5-}$) in a copper(II)-bipyridine MOF (Scheme 43) is also able to catalyze the light-mediated photocatalytic aza-Henry reaction of *N*-aryl tetrahydroisoquinolines with nitromethane in the presence of oxygen.[103] Based on control experiments using $K_5[SiW_{11}O_{39}Ru(H_2O)] \cdot 10H_2O$ as PC with and without $Cu(NO_3)_2 \cdot 3H_2O$ as co-catalyst, the authors claimed that Cu activates the nucleophile and this effect is significantly enhanced when it is directly connected to the PC through the MOF structure due to close spatial proximity.

The same group developed a MOF (Zn–PYI) that contains a stereoselective organocatalyst (L-or D-pyrollidin-2-ylimdazole) and a photocatalytically active triphenylamine moiety in the organic unit.[104] The asymmetric, photocatalytically active MOF enabled the α-alkylation of aliphatic aldehydes (**87**) with diethyl 2-bromomalonate (**31**) using visible light with high enantioselectivity (Scheme 44). More recently, the same reaction was catalyzed by a MOF where a red shift of the ligand, that contains a chromophore and an asymmetric ligand, was observed after the MOF assembly.[105] This was attributed to a

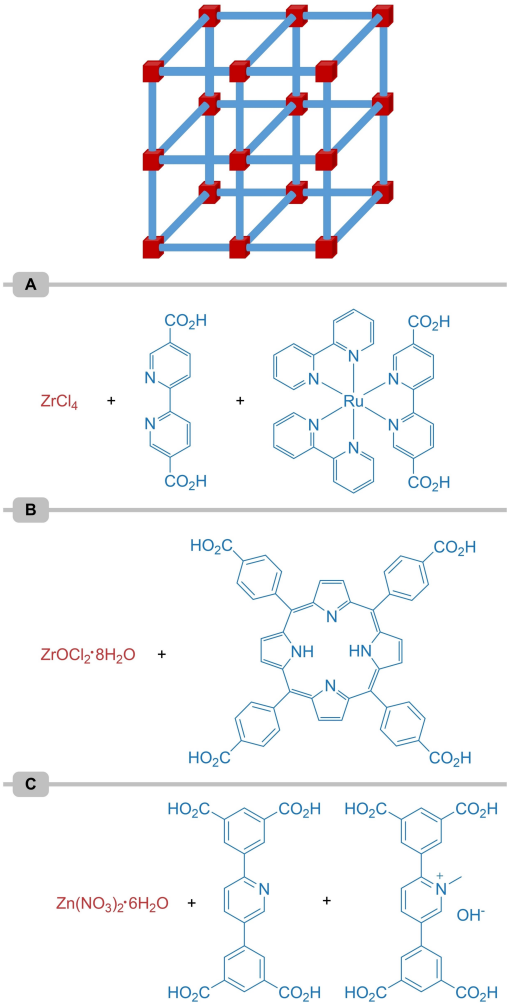

Scheme 42. Precursors for metal organic frameworks that contain a photocatalytically active linker unit. (A) Zr–MOF with Ru polypyridyl complex.[98] (B) Zr–MOF with porphyrin linker.[100] (C) Zn–MOF using a combination of two ligands.[102]

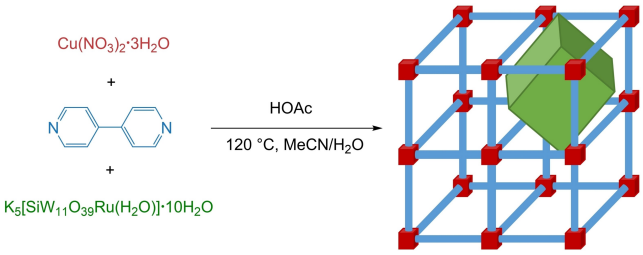

Scheme 43. Incorporation of a polyoxometalate photocatalyst in the pores of a photocatalytically inactive MOF.[103]

metal-to-ligand charge transfer between the metal (Zn, Zr or Ti) and the ligand.

Lin and co-workers combined a photoactive iridium- and a nickel complex in a zirconium MOF (Zr_{12}–Ir–Ni) and showed its use in the metallaphotoredox C–S cross-coupling of aryl iodides (**62-I**) and thiols (**13**, Scheme 45).[106] The close spatial proximity of the Ir^{III} and Ni^{II} complexes (~0.6 nm) in Zr_{12}–Ir–Ni facilitates electron and thiol radical transfers and the catalytic system

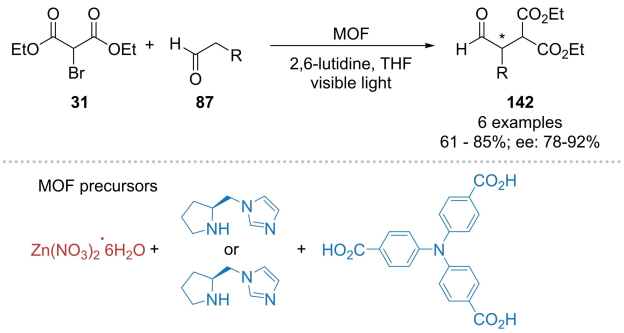

Scheme 44. Stereoselective alkylation using a MOF that contains an organocatalyst and a photoredox catalyst.[104,105]

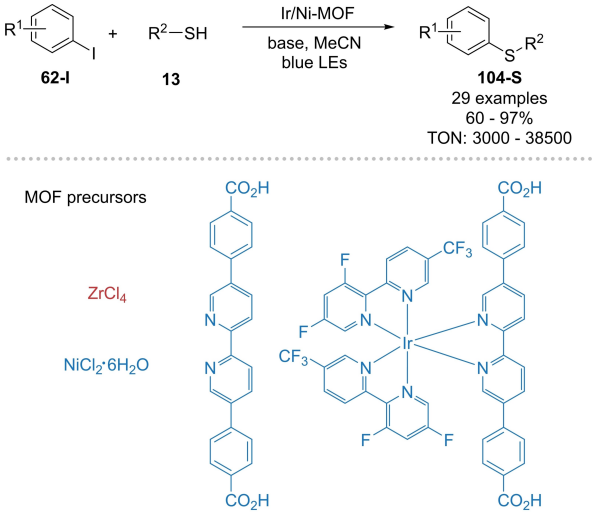

Scheme 45. Fully heterogeneous dual nickel/photocatalytic thioetherification using a Zr–MOF that contains a photocatalytically active Ir complex and a Ni complex in the organic unit.[106]

reached turnover numbers up to 38500. The system was synthesized a solvothermal reaction of $ZrCl_4$, H_2DBB and the iridium complex, and post-synthetic metalation with $NiCl_2 \cdot 6H_2O$.

More recently, a two-dimensional metal organic layer was constructed using Hafnium clusters that are bridged by photocatalytically active iridium complexes (Scheme 46).[107] The metal-organic layers were functionalized with a nickel complex, resulting in a single material that is capable of catalysing the cross-coupling reactions of aryl halides (62) with thiols (98-S), alcohols (98-O), or potassium trifluoroborates (144). The fully heterogeneous dual catalyst was recycled five times without losing its catalytic activity and only low amounts of leached Hf (<0.3%), Ir (<0.6%) and Ni (<0.1%) were determined by ICP-OES.

10. Conclusions

A variety of heterogeneous materials has been employed as recyclable photocatalysts for organic synthesis. Inorganic semi-

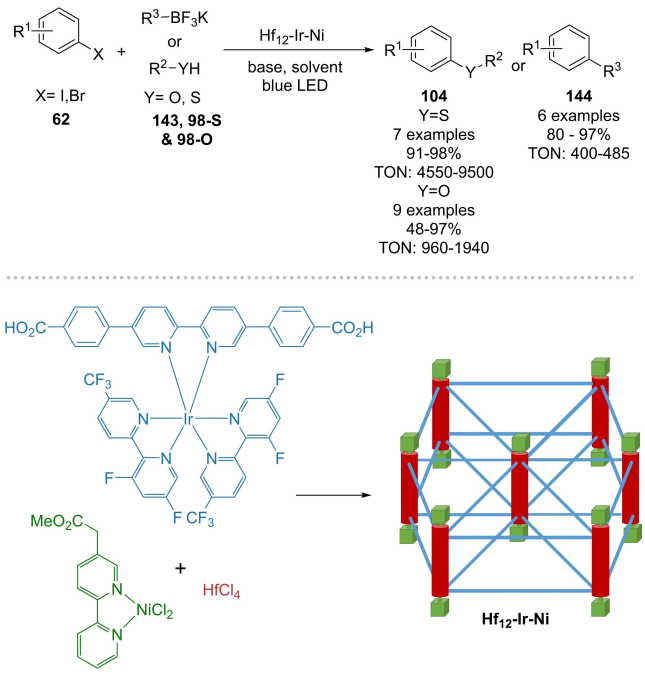

Scheme 46. Fully heterogeneous dual nickel/photocatalytic C–O, C–S and C–C cross-couplings using a Hf–MOF that contains a photocatalytically active Ir complex and a Ni complex in the organic unit.[107]

conductors, especially TiO_2, are most commonly used to replace homogeneous photocatalysts. Surface complexation, dye sensitization and doping are common methods to enable the wide-band gap semiconductor to harvest visible light up to near IR, which is rarely reached by homogeneous photocatalysts. The combination of photocatalysts with heterogeneous nanoparticles that are capable of photon upconversion is an alternative strategy for accessing near IR light and might be a promising concept for, for example, the application of photocatalysis in *in vivo* experiments.[108]

However, apart from other inorganic semiconductors, purely organic semiconductors of the carbon nitride family have rapidly emerged to a useful alternative that harvest visible light without the need for doping. The straightforward preparation of these classical semiconductors from cheap starting materials is one of the main advantages. It was also shown that semiconductor photocatalysis could be used in synergy with other catalytic reactions in dual catalytic processes.

More recently, polymeric porous materials that include conjugated microporous polymers, covalent organic frameworks and metal organic frameworks are slowly implemented in photocatalytic organic transformations. The main advantage of these materials is their rational design. Their precise preparation using, for example, cross couplings enables straightforward tuning of their electrical and optical properties. Moreover, the incorporation of a photocatalytic unit and a second catalyst accesses a single, recyclable material that enables dual catalytic processes.

As each heterogeneous photocatalyst has advantages and disadvantages, the decision for the best material has to be made case-by-case considering the respective reaction, the reaction scale and the available light source. A problem that all heterogeneous photocatalysts have in common is their limited applicability for large-scale reactions. This problem is easy to address for homogeneous photocatalysis using flow technologies, but challenging for semiconductors and only a few approaches exist. It is therefore important to note that research in heterogeneous photocatalysis should not only focus on new transformations and improved catalysts, but also needs dedicated technologies for their applications.

Acknowledgments

We gratefully acknowledge the Max-Planck Society for generous financial support. S.G. and B.P. thank the International Max Planck Research School on Multiscale Bio-Systems for funding. B. P. acknowledge financial support by a Liebig Fellowship of the German Chemical Industry Fund (Fonds der Chemischen Industrie, FCI). B.P. thanks the Deutsche Forschungsgemeinschaft (DFG, German Research Foundation) under Germany's Excellence Strategy – EXC 2008/1 – 390540038.

Conflict of Interest

The authors declare no conflict of interest.

Keywords: conjugated microporous polymers · covalent organic frameworks · heterogeneous photocatalysis · metal organic frameworks · semiconductors

[1] D. J. Cole-Hamilton, *Science* **2003**, *299*, 1702–1706.
[2] S. Hübner, J. G. de Vries, V. Farina, *Adv. Synth. Catal.* **2016**, *358*, 3–25.
[3] a) D. M. Schultz, T. P. Yoon, *Science* **2014**, *343*, 1239176; b) L. Marzo, S. K. Pagire, O. Reiser, B. König, *Angew. Chem. Int. Ed.* **2018**, *57*, 10034–10072; c) R. C. McAtee, E. J. McClain, C. R. J. Stephenson, *Trends Chem.* **2019**, *1*, 111–125; d) C. Cavedon, P. H. Seeberger, B. Pieber, *Eur. J. Org. Chem.*, DOI: 10.1002/ejoc.201901173.
[4] a) F. Strieth-Kalthoff, M. J. James, M. Teders, L. Pitzer, F. Glorius, *Chem. Soc. Rev.* **2018**, *47*, 7190–7202; b) Q.-Q. Zhou, Y.-Q. Zou, L.-Q. Lu, W.-J. Xiao, *Angew. Chem. Int. Ed.* **2019**, *58*, 1586–1604.
[5] a) D. Friedmann, A. Hakki, H. Kim, W. Choi, D. Bahnemann, *Green Chem.* **2016**, *18*, 5391–5411; b) X. Lang, X. Chen, J. Zhao, *Chem. Soc. Rev.* **2014**, *43*, 473–486.
[6] a) J. Guerra, D. Cantillo, C. O. Kappe, *Catal. Sci. Technol.* **2016**, *6*, 4695–4699; b) W.-J. Yoo, S. Kobayashi, *Green Chem.* **2014**, *16*, 2438–2442; c) J. Ma, F. Strieth-Kalthoff, T. Dalton, M. Freitag, J. L. Schwarz, K. Bergander, C. Daniliuc, F. Glorius, *Chem* **2019**, *5*, 2854–2864; d) Z. Amara, J. F. B. Bellamy, R. Horvath, S. J. Miller, A. Beeby, A. Burgard, K. Rossen, M. Poliakoff, M. W. George, *Nat. Chem.* **2015**, *7*, 489–495.
[7] a) P. Riente, T. Noël, *Catal. Sci. Technol.* **2019**, *9*, 5186–5232; b) A. Savateev, I. Ghosh, B. König, M. Antonietti, *Angew. Chem. Int. Ed.* **2018**, *57*, 15936–15947; c) A. Savateev, M. Antonietti, *ACS Catal.* **2018**, *8*, 9790–9808; d) Y. Markushyna, C. A. Smith, A. Savateev, *Eur. J. Org. Chem.*, DOI: 10.1002/ejoc.201901112; e) N. Chaoui, M. Trunk, R. Dawson, J. Schmidt, A. Thomas, *Chem. Soc. Rev.* **2017**, *46*, 3302–3321; f) J. Schneider, M. Matsuoka, M. Takeuchi, J. Zhang, Y. Horiuchi, M. Anpo, D. W. Bahnemann, *Chem. Rev.* **2014**, *114*, 9919–9986.
[8] a) N. Hoffmann, *Aust. J. Chem.* **2015**, *68*, 1621–1639; b) H. Cheng, W. Xu, *Org. Biomol. Chem.* **2019**, *17*, 9977–9989.
[9] D. W. Manley, R. T. McBurney, P. Miller, J. C. Walton, A. Mills, C. O'Rourke, *J. Org. Chem.* **2014**, *79*, 1386–1398.

[10] J. Zoller, D. C. Fabry, M. Rueping, *ACS Catal.* **2015**, *5*, 3900–3904.
[11] C. Vila, M. Rueping, *Green Chem.* **2013**, *15*, 2056–2059.
[12] C. Bottecchia, N. Erdmann, P. M. A. Tijssen, L.-G. Milroy, L. Brunsveld, V. Hessel, T. Noël, *ChemSusChem* **2016**, *9*, 1781–1785.
[13] a) M. B. Plutschack, B. Pieber, K. Gilmore, P. H. Seeberger, *Chem. Rev.* **2017**, *117*, 11796–11893; b) D. Cambié, C. Bottecchia, N. J. W. Straathof, V. Hessel, T. Noël, *Chem. Rev.* **2016**, *116*, 10276–10341.
[14] V. T. Bhat, P. A. Duspara, S. Seo, N. S. B. Abu Bakar, M. F. Greaney, *Chem. Commun.* **2015**, *51*, 4383–4385.
[15] S. P. Pitre, T. P. Yoon, J. C. Scaiano, *Chem. Commun.* **2017**, *53*, 4335–4338.
[16] S. P. Pitre, J. C. Scaiano, T. P. Yoon, *ACS Catal.* **2017**, *7*, 6440–6444.
[17] A. Hagfeldt, G. Boschloo, L. Sun, L. Kloo, H. Pettersson, *Chem. Rev.* **2010**, *110*, 6595–6663.
[18] J. Willkomm, K. L. Orchard, A. Reynal, E. Pastor, J. R. Durrant, E. Reisner, *Chem. Soc. Rev.* **2016**, *45*, 9–23.
[19] L. Zhang, J. M. Cole, *ACS Appl. Mater. Interfaces* **2015**, *7*, 3427–3455.
[20] Y. Ooyama, Y. Harima, *ChemPhysChem* **2012**, *13*, 4032–4080.
[21] M. Zhang, C. Chen, W. Ma, J. Zhao, *Angew. Chem. Int. Ed.* **2008**, *47*, 9730–9733; *Angew. Chem.* **2008**, *120*, 9876–9879.
[22] Y. Zhang, Z. Wang, X. Lang, *Catal. Sci. Technol.* **2017**, *7*, 4955–4963.
[23] X. Li, J.-L. Shi, H. Hao, X. Lang, *Appl. Catal. B* **2018**, *232*, 260–267.
[24] X. Lang, J. Zhao, X. Chen, *Angew. Chem. Int. Ed.* **2016**, *55*, 4697–4700; *Angew. Chem.* **2016**, *128*, 4775–4778.
[25] L. Ren, M.-M. Yang, C.-H. Tung, L.-Z. Wu, H. Cong, *ACS Catal.* **2017**, *7*, 8134–8138.
[26] M. Hosseini-Sarvari, M. Koohgard, S. Firoozi, A. Mohajeri, H. Tavakolian, *New J. Chem.* **2018**, *42*, 6880–6888.
[27] A. M. Nauth, E. Schechtel, R. Doren, W. Tremel, T. Opatz, *J. Am. Chem. Soc.* **2018**, *140*, 14169–14177.
[28] a) M. N. Hopkinson, B. Sahoo, J.-L. Li, F. Glorius, *Chem. Eur. J.* **2014**, *20*, 3874–3886; b) K. L. Skubi, T. R. Blum, T. P. Yoon, *Chem. Rev.* **2016**, *116*, 10035–10074.
[29] M. Cherevatskaya, M. Neumann, S. Füldner, C. Harlander, S. Kümmel, S. Dankesreiter, A. Pfitzner, K. Zeitler, B. König, *Angew. Chem. Int. Ed.* **2012**, *51*, 4062–4066; *Angew. Chem.* **2012**, *124*, 4138–4142.
[30] H.-S. Yoon, X.-H. Ho, J. Jang, H.-J. Lee, S.-J. Kim, H.-Y. Jang, *Org. Lett.* **2012**, *14*, 3272–3275.
[31] J. Tang, G. Grampp, Y. Liu, B.-X. Wang, F.-F. Tao, L.-J. Wang, X.-Z. Liang, H.-Q. Xiao, Y.-M. Shen, *J. Org. Chem.* **2015**, *80*, 2724–2732.
[32] G. K. Hodgson, J. C. Scaiano, *ACS Catal.* **2018**, *8*, 2914–2922.
[33] A. E. Lanterna, A. Elhage, J. C. Scaiano, *Catal. Sci. Technol.* **2015**, *5*, 4336–4340.
[34] N. Marina, A. E. Lanterna, J. C. Scaiano, *ACS Catal.* **2018**, *8*, 7593–7597.
[35] A. Elhage, A. E. Lanterna, J. C. Scaiano, *ACS Sustainable Chem. Eng.* **2018**, *6*, 1717–1722.
[36] L. Buglioni, P. Riente, E. Palomares, M. A. Pericàs, *Eur. J. Org. Chem.* **2017**, *2017*, 6986–6990.
[37] O. O. Fadeyi, J. J. Mousseau, Y. Feng, C. Allais, P. Nuhant, M. Z. Chen, B. Pierce, R. Robinson, *Org. Lett.* **2015**, *17*, 5756–5759.
[38] P. Riente, M. A. Pericàs, *ChemSusChem* **2015**, *8*, 1841–1844.
[39] P. Riente, A. Matas Adams, J. Albero, E. Palomares, M. A. Pericàs, *Angew. Chem. Int. Ed.* **2014**, *53*, 9613–9616; *Angew. Chem.* **2014**, *126*, 9767–9770.
[40] a) Y. Zhang, Y.-J. Xu, *RSC Adv.* **2014**, *4*, 2904–2910; b) Y. Zhang, N. Zhang, Z.-R. Tang, Y.-J. Xu, *Chem. Sci.* **2013**, *4*, 1820–1824.
[41] X. Cao, Z. Chen, R. Lin, W.-C. Cheong, S. Liu, J. Zhang, Q. Peng, C. Chen, T. Han, X. Tong, Y. Wang, R. Shen, W. Zhu, D. Wang, Y. Li, *Nat. Catal.* **2018**, *1*, 704–710.
[42] a) Y. Wu, B. Yuan, M. Li, W.-H. Zhang, Y. Liu, C. Li, *Chem. Sci.* **2015**, *6*, 1873–1878; b) B. Yuan, R. Chong, B. Zhang, J. Li, Y. Liu, C. Li, *Chem. Commun.* **2014**, *50*, 15593–15596.
[43] A. D. Yoffe, *Adv. Phys.* **2001**, *50*, 1–208.
[44] M. J. Enright, K. Gilbert-Bass, H. Sarsito, B. M. Cossairt, *Chem. Mater.* **2019**, *31*, 2677–2682.
[45] Y. Jiang, C. Wang, C. R. Rogers, M. S. Kodaimati, E. A. Weiss, *Nat. Chem.* **2019**, *11*, 1034–1040.
[46] C. Liu, Z. Chen, C. Su, X. Zhao, Q. Gao, G.-H. Ning, H. Zhu, W. Tang, K. Leng, W. Fu, B. Tian, X. Peng, J. Li, Q.-H. Xu, W. Zhou, K. P. Loh, *Nat. Commun.* **2018**, *9*, 80.
[47] A. Pal, I. Ghosh, S. Sapra, B. König, *Chem. Mater.* **2017**, *29*, 5225–5231.
[48] J. A. Caputo, L. C. Frenette, N. Zhao, K. L. Sowers, T. D. Krauss, D. J. Weix, *J. Am. Chem. Soc.* **2017**, *139*, 4250–4253.
[49] Y.-Y. Liu, D. Liang, L.-Q. Lu, W.-J. Xiao, *Chem. Commun.* **2019**, *55*, 4853–4856.
[50] Z. Zhang, K. Edme, S. Lian, E. A. Weiss, *J. Am. Chem. Soc.* **2017**, *139*, 4246–4249.
[51] W. Zhao, C. Liu, L. Cao, X. Yin, H. Xu, B. Zhang, *RSC Adv.* **2013**, *3*, 22944–22948.
[52] Z.-W. Xi, L. Yang, D.-Y. Wang, C.-D. Pu, Y.-M. Shen, C.-D. Wu, X.-G. Peng, *J. Org. Chem.* **2018**, *83*, 11886–11895.
[53] B. Saparov, D. B. Mitzi, *Chem. Rev.* **2016**, *116*, 4558–4596.
[54] W.-B. Wu, Y.-C. Wong, Z.-K. Tan, J. Wu, *Catal. Sci. Technol.* **2018**, *8*, 4257–4263.
[55] X. Zhu, Y. Lin, Y. Sun, M. C. Beard, Y. Yan, *J. Am. Chem. Soc.* **2019**, *141*, 733–738.
[56] X. Zhu, Y. Lin, J. San Martin, Y. Sun, D. Zhu, Y. Yan, *Nat. Commun.* **2019**, *10*, 2843.
[57] W.-J. Ong, L.-L. Tan, Y. H. Ng, S.-T. Yong, S.-P. Chai, *Chem. Rev.* **2016**, *116*, 7159–7329.
[58] F. Su, S. C. Mathew, G. Lipner, X. Fu, M. Antonietti, S. Blechert, X. Wang, *J. Am. Chem. Soc.* **2010**, *132*, 16299–16301.
[59] F. Su, S. C. Mathew, L. Möhlmann, M. Antonietti, X. Wang, S. Blechert, *Angew. Chem. Int. Ed.* **2011**, *50*, 657–660; *Angew. Chem.* **2011**, *123*, 683–686.
[60] L. Möhlmann, M. Baar, J. Rieß, M. Antonietti, X. Wang, S. Blechert, *Adv. Synth. Catal.* **2012**, *354*, 1909-1913.
[61] M. Baar, S. Blechert, *Chem. Eur. J.* **2015**, *21*, 526–530.
[62] I. Ghosh, J. Khamrai, A. Savateev, N. Shlapakov, M. Antonietti, B. König, *Science* **2019**, *365*, 360–366.
[63] a) B. Pieber, J. A. Malik, C. Cavedon, S. Gisbertz, A. Savateev, D. Cruz, T. Heil, G. Zhang, P. H. Seeberger, *Angew. Chem. Int. Ed.* **2019**, *58*, 9575–9580; b) C. Cavedon, A. Madani, P. H. Seeberger, B. Pieber, *Org. Lett.* **2019**, *21*, 5331–5334; c) S. Gisbertz, S. Reischauer, B. Pieber, *ChemRxiv*, preprint, DOI 10.26434/chemrxiv.10298735.v10298731.
[64] Y. Cai, Y. Tang, L. Fan, Q. Lefebvre, H. Hou, M. Rueping, *ACS Catal.* **2018**, *8*, 9471–9476.
[65] A. Vijeta, E. Reisner, *Chem. Commun.* **2019**, *55*, 14007–14010.
[66] A. U. Meyer, V. W. H. Lau, B. Konig, B. V. Lotsch, *Eur. J. Org. Chem.* **2017**, 2179–2185.
[67] B. Pieber, M. Shalom, M. Antonietti, P. H. Seeberger, K. Gilmore, *Angew. Chem. Int. Ed.* **2018**, *57*, 9976–9979.
[68] B. Kurpil, K. Otte, M. Antonietti, A. Savateev, *Appl. Catal. B* **2018**, *228*, 97–102.
[69] B. Kurpil, K. Otte, A. Mishchenko, P. Lamagni, W. Lipiński, N. Lock, M. Antonietti, A. Savateev, *Nat. Commun.* **2019**, *10*, 945.
[70] B. Kurpil, Y. Markushyna, A. Savateev, *ACS Catal.* **2019**, *9*, 1531–1538.
[71] R. Li, J. Byun, W. Huang, C. Ayed, L. Wang, K. A. I. Zhang, *ACS Catal.* **2018**, *8*, 4735–4750.
[72] K. Zhang, D. Kopetzki, P. H. Seeberger, M. Antonietti, F. Vilela, *Angew. Chem. Int. Ed.* **2013**, *52*, 1432–1436; *Angew. Chem.* **2013**, *125*, 1472–1476.
[73] E. R. Welin, C. Le, D. M. Arias-Rotondo, J. K. McCusker, D. W. C. MacMillan, *Science* **2017**, *355*, 380–385.
[74] Z. J. Wang, S. Ghasimi, K. Landfester, K. A. I. Zhang, *Chem. Commun.* **2014**, *50*, 8177–8180.
[75] L. Ma, Y. Liu, Y. Liu, S. Jiang, P. Li, Y. Hao, P. Shao, A. Yin, X. Feng, B. Wang, *Angew. Chem. Int. Ed.* **2019**, *58*, 4221–4226.
[76] Z. J. Wang, S. Ghasimi, K. Landfester, K. A. I. Zhang, *J. Mater. Chem. A* **2014**, *2*, 18720–18724.
[77] R. Li, Z. J. Wang, L. Wang, B. C. Ma, S. Ghasimi, H. Lu, K. Landfester, K. A. I. Zhang, *ACS Catal.* **2016**, *6*, 1113–1121.
[78] Z. J. Wang, S. Ghasimi, K. Landfester, K. A. I. Zhang, *Adv. Synth. Catal.* **2016**, *358*, 2576–2582.
[79] Z. J. Wang, S. Ghasimi, K. Landfester, K. A. I. Zhang, *Adv. Mater.* **2015**, *27*, 6265–6270.
[80] Z. J. Wang, S. Ghasimi, K. Landfester, K. A. I. Zhang, *Chem. Mater.* **2015**, *27*, 1921–1924.
[81] V. R. Battula, H. Singh, S. Kumar, I. Bala, S. K. Pal, K. Kailasam, *ACS Catal.* **2018**, *8*, 6751–6759.
[82] C. Su, R. Tandiana, B. Tian, A. Sengupta, W. Tang, J. Su, K. P. Loh, *ACS Catal.* **2016**, *6*, 3594–3599.
[83] J. Luo, X. Zhang, J. Zhang, *ACS Catal.* **2015**, *5*, 2250–2254.
[84] H.-P. Liang, Q. Chen, B.-H. Han, *ACS Catal.* **2018**, *8*, 5313–5322.
[85] C.-A. Wang, Y.-W. Li, X.-L. Cheng, J.-P. Zhang, Y.-F. Han, *RSC Adv.* **2017**, *7*, 408–414.
[86] W. T. Liu, S. J. Wu, Q. Su, B. X. Guo, P. Y. Ju, G. H. Li, Q. L. Wu, *J. Mater. Sci.* **2019**, *54*, 1205–1212.
[87] S. Ghasimi, S. A. Bretschneider, W. Huang, K. Landfester, K. A. I. Zhang, *Adv. Sci.* **2017**, *4*, 1700101.

[88] W. Ou, G. Zhang, J. Wu, C. Su, *ACS Catal.* **2019**, *9*, 5178–5183.
[89] C. S. Diercks, O. M. Yaghi, *Science* **2017**, *355*, eaal1585.
[90] W. Huang, B. C. Ma, H. Lu, R. Li, L. Wang, K. Landfester, K. A. I. Zhang, *ACS Catal.* **2017**, *7*, 5438–5442.
[91] Y. Zhi, Z. Li, X. Feng, H. Xia, Y. Zhang, Z. Shi, Y. Mu, X. Liu, *J. Mater. Chem. A* **2017**, *5*, 22933–22938.
[92] W. Huang, J. Byun, I. Rörich, C. Ramanan, P. W. M. Blom, H. Lu, D. Wang, L. Caire da Silva, R. Li, L. Wang, K. Landfester, K. A. I. Zhang, *Angew. Chem. Int. Ed.* **2018**, *57*, 8316–8320; *Angew. Chem.* **2018**, *130*, 8449–8453.
[93] S. Liu, W. Pan, S. Wu, X. Bu, S. Xin, J. Yu, H. Xu, X. Yang, *Green Chem.* **2019**, *21*, 2905–2910.
[94] W. Liu, Q. Su, P. Ju, B. Guo, H. Zhou, G. Li, Q. Wu, *ChemSusChem* **2017**, *10*, 664–669.
[95] R. Chen, J.-L. Shi, Y. Ma, G. Lin, X. Lang, C. Wang, *Angew. Chem. Int. Ed.* **2019**, *58*, 6430–6434.
[96] P.-F. Wei, M.-Z. Qi, Z.-P. Wang, S.-Y. Ding, W. Yu, Q. Liu, L.-K. Wang, H.-Z. Wang, W.-K. An, W. Wang, *J. Am. Chem. Soc.* **2018**, *140*, 4623–4631.
[97] L. Zeng, X. Guo, C. He, C. Duan, *ACS Catal.* **2016**, *6*, 7935–7947.
[98] C. Wang, Z. Xie, K. E. deKrafft, W. Lin, *J. Am. Chem. Soc.* **2011**, *133*, 13445–13454.
[99] X. Yu, S. M. Cohen, *J. Am. Chem. Soc.* **2016**, *138*, 12320–12323.
[100] C. Xu, H. Liu, D. Li, J.-H. Su, H.-L. Jiang, *Chem. Sci.* **2018**, *9*, 3152–3158.
[101] J. A. Johnson, J. Luo, X. Zhang, Y.-S. Chen, M. D. Morton, E. Echeverría, F. E. Torres, J. Zhang, *ACS Catal.* **2015**, *5*, 5283–5291.
[102] H. Li, Y. Yang, C. He, L. Zeng, C. Duan, *ACS Catal.* **2019**, *9*, 422–430.
[103] D. Shi, C. He, B. Qi, C. Chen, J. Niu, C. Duan, *Chem. Sci.* **2015**, *6*, 1035–1042.
[104] P. Wu, C. He, J. Wang, X. Peng, X. Li, Y. An, C. Duan, *J. Am. Chem. Soc.* **2012**, *134*, 14991–14999.
[105] Y. Zhang, J. Guo, L. Shi, Y. Zhu, K. Hou, Y. Zheng, Z. Tang, *Sci. Adv.* **2017**, *3*, e1701162.
[106] Y.-Y. Zhu, G. Lan, Y. Fan, S. S. Veroneau, Y. Song, D. Micheroni, W. Lin, *Angew. Chem. Int. Ed.* **2018**, *57*, 14090–14094.
[107] G. Lan, Y. Quan, M. Wang, G. T. Nash, E. You, Y. Song, S. S. Veroneau, X. Jiang, W. Lin, *J. Am. Chem. Soc.* **2019**, *141*, 15767–15772.
[108] M. Freitag, N. Möller, A. Rühling, C. A. Strassert, B. J. Ravoo, F. Glorius, *ChemPhotoChem* **2019**, *3*, 24–27.

Manuscript received: January 31, 2020
Revised manuscript received: February 20, 2020
Accepted manuscript online: February 21, 2020
Version of record online: March 23, 2020